Report 7, 1991

DISTRIBUTED PARAMETER MODELS THE GLERARDALUR GEOTHERMAL FIELD, N-ICELAND THE PODHALE GEOTHERMAL FIELD, S-POLAND

Maria Gladysz,
UNU Geothermal Training Programme,
Orkustofnun - National Energy Authority,
Grensasvegur 9,
108 Reykjavik,
ICELAND

Permanent address:
Polish Academy of Sciences,
Minerals and Energy Economy Research Centre,
Jozefa Wybickiego,
31-261 Krakow,
POLAND

ABSTRACT

The report describes distributed parameter models of two geothermal reservoirs. The basic equations of the problem are derived and the reservoir behaviour of two different geothermal fields is analyzed.

The first field is the Glerardalur geothermal field in N-Iceland. In this case the calibration of the model was made on the basis of 10 years of observations of the reservoir response to production. A good fit was achieved with the model for drawdown. The obtained reservoir parameters were used for future prediction of the pressure response of the field for different constant production rates. The present trend of stabilized drawdown can be maintained only for an annual average production rate not larger than 15 l/s. The calculations showed no cooling during the production period as well as for the future prediction period.

The second field is the Podhale geothermal field in S-Poland. Because of insufficient amount of data from existing wells, only the theoretical model of the field was tested. The reservoir parameters chosen are believed to be close to real values. A stationary flow problem was solved for various constant production rates, as well as the transient heat transport problem, in order to determine the break-through time for the cold front. Two cases were examined: one consisting of one geothermal doublet (one production well and one injection well) and the other of five doublets in operation. The model shows that there is almost no difference in drawdown in both cases. Assuming production does not exceed the present artesian outflow of 20 l/s, the predicted temperature decline in production wells after 50 years of operation is less than 2°C. For the smallest distance between the wells, 710 m, the expected breakthrough time is 400 years.

TABLE OF CONTENTS

Page

ABSTRACT 3

TABLE OF CONTENTS 4

LIST OF FIGURES 5

LIST OF TABLES 5

1. INTRODUCTION 6

2. DISTRIBUTED PARAMETER MODEL 7
   2.1 General overview 7
   2.2 Theoretical basis with emphasis on the AQUA programme package 7
      2.2.1 Flow model 7
      2.2.2 Mass transport model 8
      2.2.3 Heat transport model 9

3. THE GLERARDALUR GEOTHERMAL FIELD 11
   3.1 The main features of the Glerardalur geothermal field 11
      3.1.1 Locality 11
      3.1.2 Geology and geophysics 11
      3.1.3 Production history and utilization 13
   3.2 Basic assumptions and initial parameter values of the model 14
   3.3 Results from the calibration of the reservoir parameters 15
   3.4 Future prediction of the reservoir response 20
   3.5 Conclusions and recommendations 22

4. THE PODHALE GEOTHERMAL FIELD 23
   4.1 Main features of the Podhale geothermal field 23
      4.1.1 Locality 23
      4.1.2 Geology 23
      4.1.3 Exploration and development history 23
   4.2 Basis assumptions of the Podhale model parameters 24
   4.3 Results from the flow model 26
      4.3.1 The one doublet case 26
      4.3.2 The five doublet case 29
   4.4 Results from the heat transport model 29
   4.5 Conclusions and recommendations 34

ACKNOWLEDGEMENTS 36

NOMENCLATURE 37

REFERENCES 38

LIST OF FIGURES

Page

1. General location of the Glerardalur geothermal field 11
2. Geological map of the Glerardalur geothermal field 12
3. Resistivity map of the Glerardalur geothermal field at 400 m depth 13
4. Location of wells in Glerardalur 14
5. Map of transmissivity in the vicinity of the wells 16
6. Measured and calculated drawdown, well Gy-7 17
7. Measured and calculated drawdown, well Gy-5 17
8. Measured and calculated drawdown, well Gy-8 18
9. Drawdown and flow field in the vicinity of the wells 18
10. Cross-section of the drawdown 19
11. Silica concentration and temperature decline in well Gy-7 19
12. Future prediction of the drawdown, well Gy-7 20
13. Future prediction of the drawdown, well Gy-5 20
14. Future prediction of the drawdown, well Gy-8 21
15. Future prediction of the silica concentration, well Gy-7 21
16. Future prediction of the temperature, well Gy-7 22
17. General location of the Podhale geothermal field 23
18. A simplified geological cross-section of the Podhale basin 24
19. Map of transmissivity for the distributed parameter model, Podhale 25
20. Location of wells in the Podhale model 26
21. Map of transmissivity in the vicinity of the wells, case 1 27
22. Drawdown and flow field, case 1 a 27
23. Drawdown and flow field, case 1 b 28
24. Drawdown and flow field, case 1 c 28
25. Map of transmissivity in the vicinity of the wells, case 2 29
26. Drawdown and flow field, case 2 a 30
27. Drawdown and flow field, case 2 b 30
28. Temperature decline in the production well, case 1 31
29. Temperature decline in the production wells, case 2 33
30. Map of temperature after 50 years of production, case 2 35

LIST OF TABLES

1. Average annual production and extracted energy after cooling of the water down to 30°C 14
2. Temperature decline in the production well, case 1 31
3. Breakthrough time, case 1 32
4. Temperature decline in the production wells, case 2 34
5. Breakthrough time, case 2 34

1. INTRODUCTION

The author of this report had the privilege to participate in the six months' training course of the UNU Geothermal Training Programme at Orkustofnun (the National Energy Authority) in Reykjavik, Iceland in 1991. The programme consisted of a 5 weeks' introductory lecture course, 4 weeks of specialized lectures and practical training, a field excursion lasting 8 days and three months of practical and theoretical research. The introductory course consisted of various aspects of exploration, production and utilization of geothermal energy. The most important low and high temperature geothermal fields in Iceland were visited during the field excursion. The main purpose of the research study was to obtain knowledge and skill in modelling geothermal reservoirs and in predicting their future behaviour. A detailed conceptual model of the reservoir is very important in planning the exploration, development and utilization of the geothermal energy.

The main scope of the study was the calibration of reservoir parameter values and the prediction of the future response of the reservoirs due to different production rates. The calibration and prediction processes were performed by using the numerical AQUA programme package developed by Vatnaskil Consulting Engineers.

2. DISTRIBUTED PARAMETER MODEL

2.1 General overview

Various methods are available for estimating the generating potential of the geothermal systems. The distributed parameter (numerical) model is one of them. The distributed parameter model is a general mathematical model that can be used to simulate a geothermal reservoir in as much detail as desired. If only a few grid blocks are used, one has the equivalent of the lumped parameter model, but several hundred or thousand grid blocks can be used to simulate the entire geothermal system, including the main reservoir, the confining layers, recharge zones, etc. The distributed parameter model is most useful as a reservoir evaluation tool, when some exploitation history is available (Bodvarsson and Witherspoon, 1989). The basic equations solved in distributed parameter models are mass and energy conservation equations.

2.2 Theoretical basis with emphasis on the AQUA programme package

The AQUA programme package developed by Vatnaskil Consulting Engineers (1990) solves groundwater flow and transport equations using the Galerkin finite element method. The following differential equation is the basis for the mathematical model:

$$a\frac{\delta u}{\delta t} + b_i\frac{\delta u}{\delta x_i} + \frac{\delta}{\delta x_i}(e_{ij}\frac{\delta u}{\delta x_j}) + fu + g = 0 \qquad (1)$$

The model is two dimensional, and indices i and j indicate the x and y coordinate axes.

AQUA can be used on IBM PC/XT/AT or compatible computers and requires 640 K memory RAM, EGA graphics card and display, hard disk, maths coprocessor and optional hardware: digitizer, mouse, printer, HP- plotter.

2.2.1 Flow model

For a transient groundwater flow, Equation 1 reduces to

$$a\frac{\delta u}{\delta t} + \frac{\delta}{\delta x_i}(e_{ij}\frac{\delta u}{\delta x_j}) + fu + g = 0 \qquad (2)$$

For a confined groundwater flow in a leaky aquifer, the parameters in Equation 2 are defined as:

$$u = h; \quad e_{ij} = T_{ij}; \quad f = 0; \quad g = Q + (k/m)(h_o - h); \quad a = -S$$

By using x and y instead of the indices Equation 2 then reads:

$$\frac{\delta}{\delta x}(T_{xx}\frac{\delta h}{\delta x}) + \frac{\delta}{\delta y}(T_{yy}\frac{\delta h}{\delta y}) + \frac{k}{m}(h_o - h) + Q = S\frac{\delta h}{\delta t} \qquad (3)$$

where

h - *groundwater head (m)*
T_{xx} - *transmissivity along principal axis (m^2/s)*
T_{yy} - *transmissivity perpendicular to the principal axis (m^2/s)*

Q - pumping/injection rate (m^3/s)
k/m - leakage coefficient, where k is the permeability of the semipermeable layer and m its thickness, (s^{-1})
h_o - head in upper aquifer (m)
S - storage coefficient

For long term exploitation, storage in the reservoir is controlled by compressibility of the water and the rock in terms of the elastic storage coefficient as in confined aquifers and by the delayed yield effect. In this case, the equation for the transient groundwater flow is:

$$\frac{\delta}{\delta x}(T_{xx}\frac{\delta h}{\delta x})+\frac{\delta}{\delta y}(T_{yy}\frac{\delta h}{\delta y})+\frac{k}{m}(h_o-h)+Q = S\frac{\delta h}{\delta t}+\alpha\varphi\int_0^t\frac{\delta h}{\delta t}e^{-\alpha(t-\tau)}d\tau \qquad (4)$$

where

φ - effective porosity
$\alpha = 1/\kappa$, and κ is a time constant (s)

For steady-state, Equation 1 reduces to

$$\frac{\delta}{\delta x_i}(e_{ij}\frac{\delta u}{\delta x_j}) + fu + g = 0 \qquad (5)$$

where we define

$u = h$; $e_{ij} = T_{ij}$; $f = 0$; $g = Q + \gamma$ and
$\gamma = R$ (infiltration rate) for a unconfined horizontal aquifer (mm/year), or
$\gamma = (k/m)(h_o-h)$ for a confined horizontal aquifer (m/s)

By using x and y instead of the indices, Equation 5 then reads:

$$\frac{\delta}{\delta x}(T_{xx}\frac{\delta h}{\delta x})+\frac{\delta}{\delta y}(T_{yy}\frac{\delta h}{\delta y})+Q+\gamma = 0 \qquad (6)$$

In the AQUA model, the following boundary conditions are allowed:

- Dirichlet boundary condition, the groundwater level, the piezometric head or the potential function is prescribed at the boundary.
- Von Neumann boundary condition, the flow at the boundary is prescribed by defining source nodes at the no-flow boundary nodes.
- Cauchy boundary condition, the boundary flow rate is related to both the normal derivative and the head.

2.2.2 Mass transport model

For the mass transport model, the parameters in Equation 1 are defined as follows:

$$u = c; \quad a = \varphi bR_d; \quad b_i = v_i b; \quad e_{ij} = -\varphi bD_{ij}; \quad f = \varphi bR_d\lambda + \gamma + Q; \quad g = -\gamma c_o - Qc_w$$

By using x and y instead of the indices, Equation 1 then reads:

$$\frac{\delta}{\delta x}(\varphi b D_{xx}\frac{\delta c}{\delta x})+\frac{\delta}{\delta y}(\varphi b D_{yy}\frac{\delta c}{\delta y})-v_x b\frac{\delta c}{\delta x}-v_y b\frac{\delta c}{\delta y}=$$

$$\varphi b R_d\frac{\delta c}{\delta t}+\varphi b R_d\lambda c-(c_o-c)\gamma-Q(c_w-c) \tag{7}$$

The above equation applies to a local coordinate system within each element having the main axis along the flow direction. The dispersion coefficients are defined by

$$\varphi D_{xx} = a_L v^n + D_m\varphi \tag{8}$$

$$\varphi D_{yy} = a_T v^n + D_m\varphi \tag{9}$$

The retardation coefficient R_d is given by

$$R_d = 1+\beta_c\frac{(1-\varphi)\rho_s}{\varphi\rho_l} \tag{10}$$

$$\beta_c = K_d\rho_l \tag{11}$$

where

c - solute concentration (kg/m^3)
c_o - solute concentration of vertical inflow (kg/m^3)
c_w - solute concentration of injected water (kg/m^3)
$v_x v_y$ - velocity vector taken from the solution of the flow problem (m/s)
a_L - longitudinal dispersivity (m)
a_T - transversal dispersivity (m)
v - velocity (m/s)
D_m - molecular diffusivity (m^2/s)
φ - effective porosity
Q - pumping rate (m^3/s)
b - aquifer thickness (m)
λ - expotential decay constant (s^{-1})
K_d - distribution coefficient
ρ_l - density of the liquid (kg/m^3)
ρ_s - density of the porous medium (kg/m^3)
γ - R (infiltration rate) for unconfined horizontal aquifer (mm/time unit)
γ - $(k/m)(h_o-h)$ for confined horizontal aquifer (m/s)
β_c - retardation constant

2.2.3 Heat transport model

For the heat transport model, the parameters in Equation 1 are defined as follows:

$$u = T;\quad a = \varphi b R_h;\quad b_i = v_i b;\quad e_{ij} = -bK_{ij};\quad f = \gamma + Q;\quad g = -\gamma T_o - QT_w$$

By using x and y instead of the indices Equation 1 then reads:

$$\frac{\delta}{\delta x}(bK_{xx}\frac{\delta T}{\delta x})+\frac{\delta}{\delta y}(bK_{yy}\frac{\delta T}{\delta y})-v_x b\frac{\delta T}{\delta x}-v_y b\frac{\delta T}{\delta y}=\varphi bR_h\frac{\delta T}{\delta t}-(T_o-T)\gamma-(T_w-T)Q \qquad (12)$$

The above equation also applies to a local coordinate system within each element having the main axis along the flow direction.

The heat dispersion coefficients are given by

$$K_{xx}=a_L v^n+D_h\varphi \qquad (13)$$

$$K_{yy}=a_T v^n+D_h\varphi \qquad (14)$$

The heat retardation coefficient R_h is given by

$$R_h=1+\beta_h\frac{(1-\varphi)\rho_s}{\varphi\rho_l} \qquad (15)$$

$$\beta_h=\frac{C_s}{C_l} \qquad (16)$$

where

T - temperature (°C)
T_o - temperature of the vertical inflow (°C)
C_l - specific heat capacity of the liquid (kJ/kg °C)
C_s - specific heat capacity of the porous medium (kJ/kg °C)
β_h - retardation constant
D_h - heat diffusivity (m^2/s)

The other parameters are defined as previously.

For both the transport models, two kinds of boundary conditions are allowed:

- Dirichlet boundary condition, the concentration or temperature is specified at the boundary.
- Von Neumann boundary condition, the concentration gradient or the temperature gradient is set to zero indicating convective transport of mass or heat through the boundary.

3. THE GLERARDALUR GEOTHERMAL FIELD

3.1 The main features of the Glerardalur geothermal field

3.1.1 Locality

The Glerardalur geothermal field is located in N-Iceland on the western outskirts of the town Akureyri. It is one of the fields supplying water to the Akureyri Municipal District Heating System. The geothermal wells are located on the western slope of the Eyjafjordur valley at an elevation of 192-308 m above sea level (Figure 1).

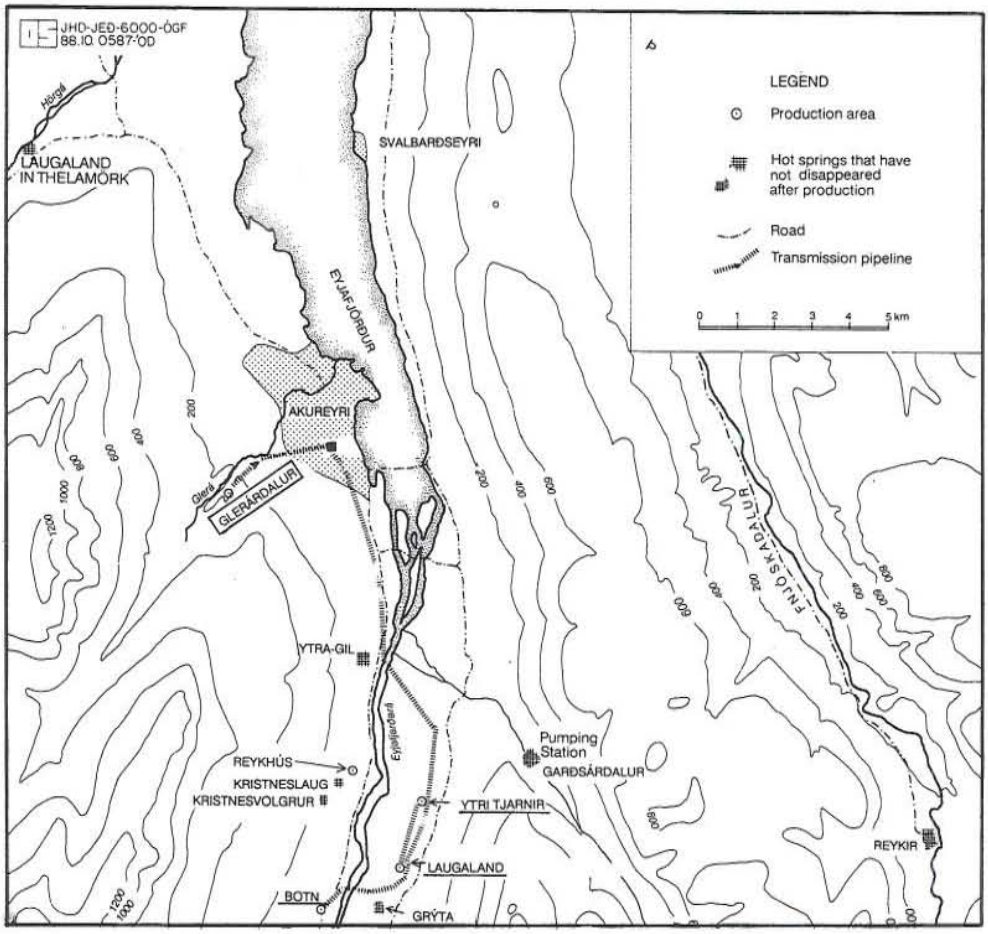

FIGURE 1: General location of the Glerardalur geothermal field

3.1.2 Geology and geophysics

Glerardalur is located in a typical Icelandic lava pile of tertiary age, close to 6 m.y. old. West of Akureyri the strike of the lava pile is east-west and its dip is to the south in the range of 3-5°. The basaltic lava at the surface is in the middle of the mesolite/scolesite alteration zone with increasing alteration with depth. Therefore, the basaltic lava pile is quite dense and of rather low permeability except in a relatively few macroscopic fractures (Flóvenz et al., 1984).

The crust in Eyjafjordur is cut by numerous near-vertical dykes and normal faults which are not active any more. The strike of the dykes and the faults is north-south (Figure 2). The geological

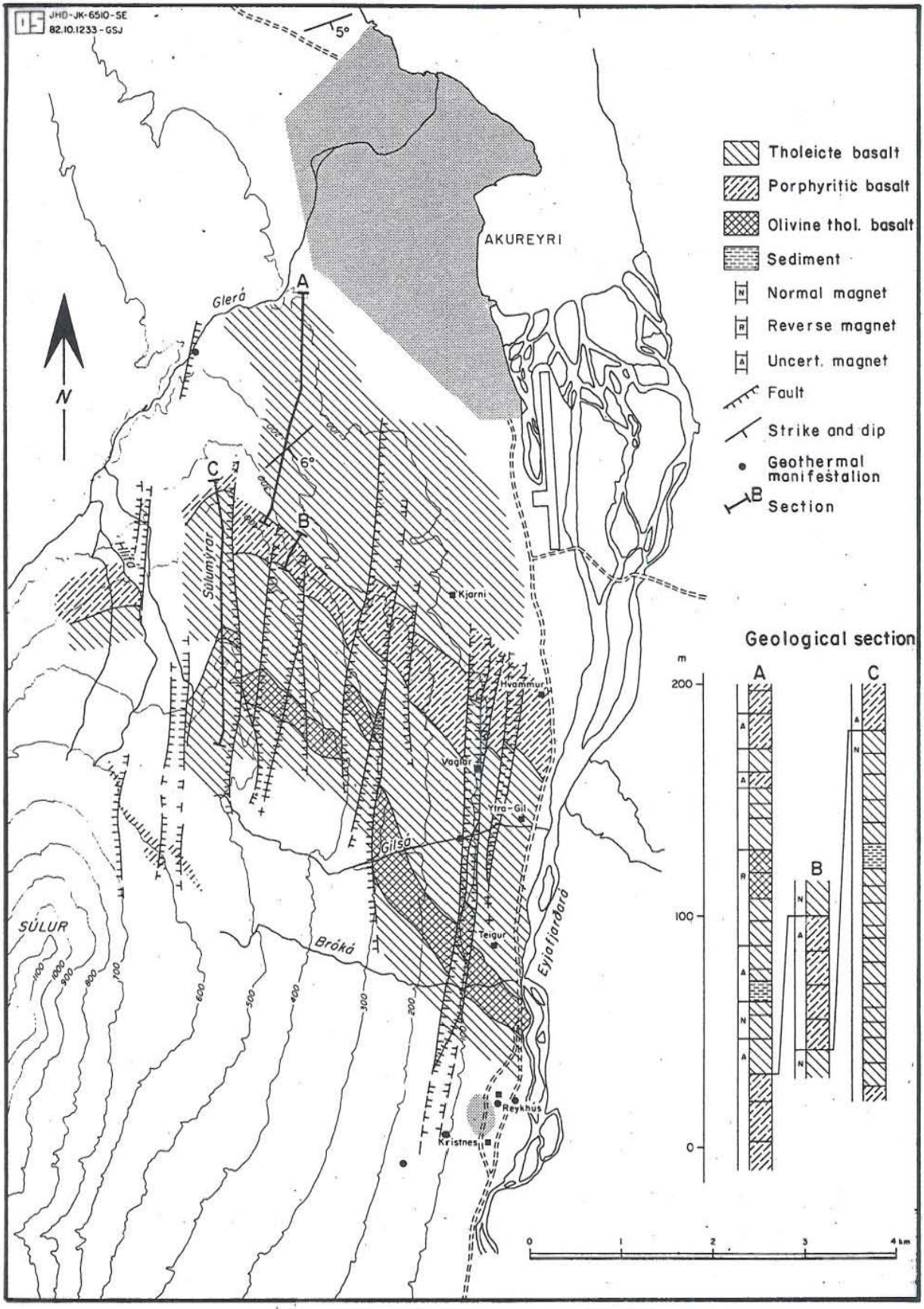

FIGURE 2: Geological map of the Glerardalur geothermal field (Flóvenz et al., 1984)

structure of the Glerardalur field was recognized by surface geological mapping as well as by a geophysical survey. Head-on resistivity profiling was mainly used. Both methods indicated the anisotropy of the strata (Figures 2 and 3).

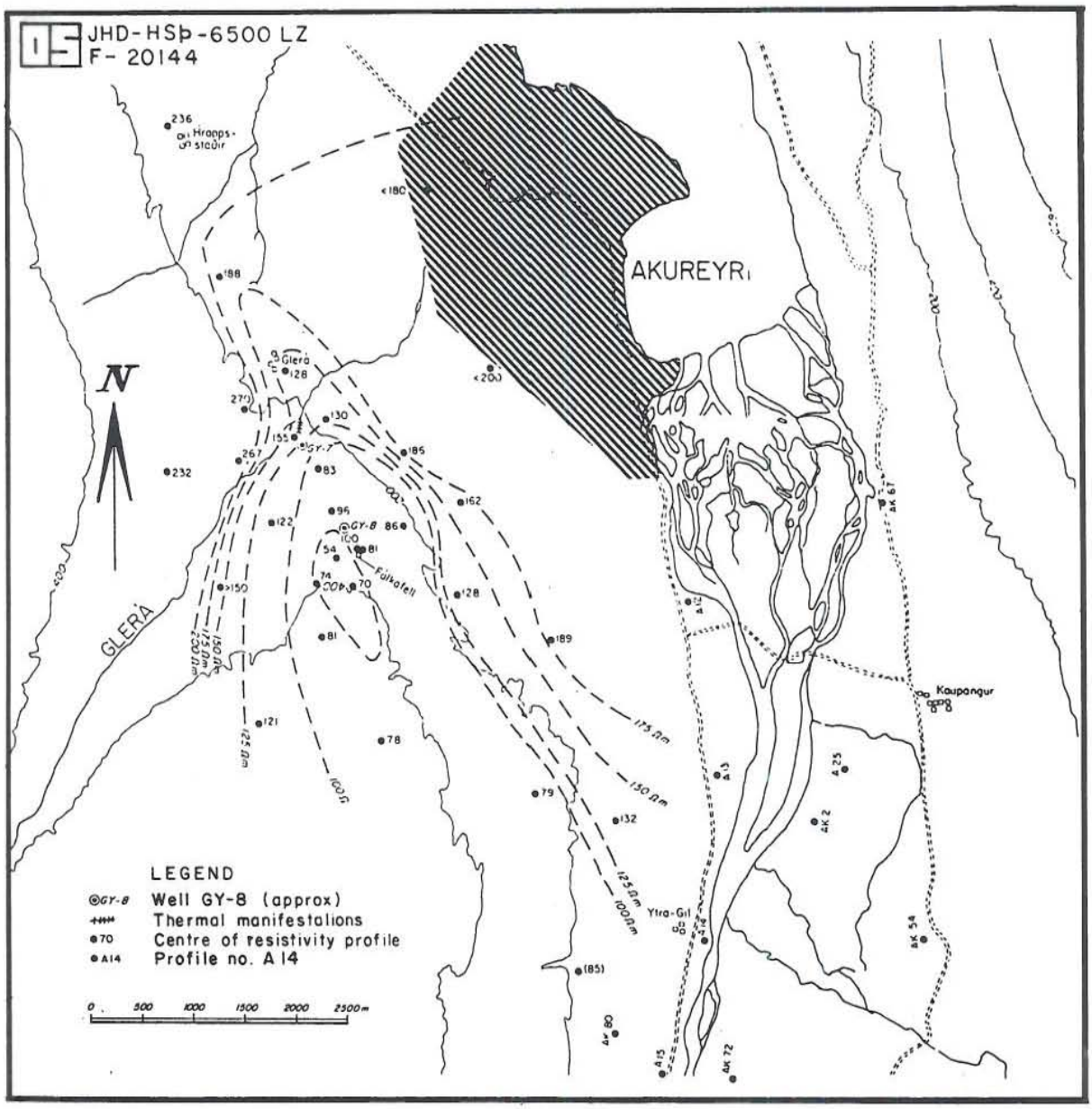

FIGURE 3: Resistivity map of the Glerardalur geothermal field at a depth of 400 m (Flóvenz et al., 1984)

3.1.3 Production history and utilization

Before any drilling took place in Glerardalur, the presence of the geothermal reservoir was manifested by several warm springs. By collecting water from the springs, a discharge of 2.5 l/s was measured. The hydrothermal system of this area is not well recognized. The recharge area is probably in the mountains to the southwest of the field and the water migrates along vertical fissures. The hot springs disappeared after production from wells started.

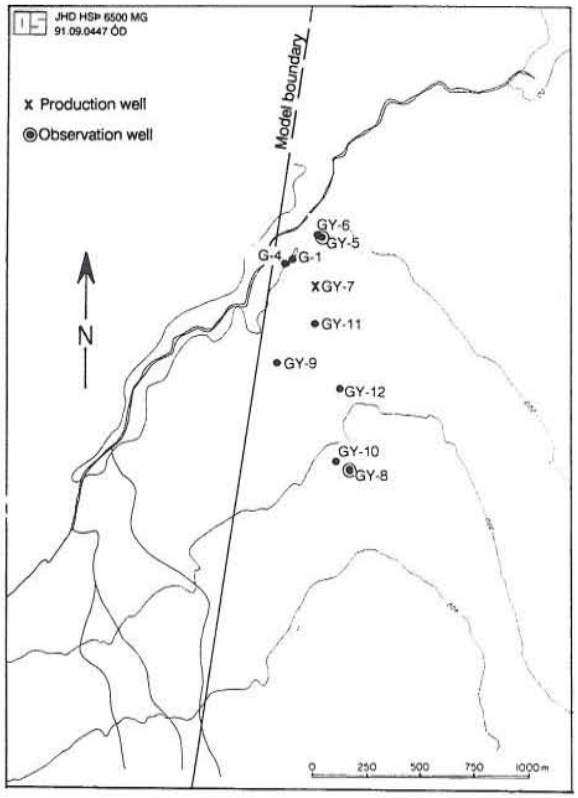

Most of the wells drilled into the reservoir are shallow (100 - 300) exploration wells (Figure 4); only one of them, Gy-7, reached the depth of 790 m. Production from the field started in 1982 and currently one well, Gy-7, is used for production. The main feed zone in the well is at a depth of 450 m and the temperature of the water is 60-61°C. The average annual production is shown in Table 1. Since 1986 production has been stopped for 2-3 months during the summer and the water level has recovered rapidly. The water from well Gy-7 is pumped directly to the central pumping station at Akureyri.

FIGURE 4: Location of wells in Glerardalur

TABLE 1: Average annual production and extracted energy after cooling of the water down to 30°C (Flóvenz et al., 1991)

Year	Production rate (l/s)	Extracted energy (GWh)
1981	3.3	3.6
1982	23.4	25.8
1983	30.0	33.0
1984	27.3	30.0
1985	23.1	25.4
1986	18.8	20.7
1987	15.6	17.2
1988	15.3	16.8
1989	13.5	14.8
1990	15.9	17.4

3.2 Basic assumptions and initial parameter values of the model

The total area covered by the model is 200 km^2. Production rates from well Gy-7 with flow rates on a weekly basis since May 1981 were used in the simulation. Observed water levels in wells Gy-7, Gy-5 and Gy-8 were matched with calculated values in the calibration process. No-flow

boundary conditions were used at all boundaries because there is no information indicating any influence far away from the production well. The western boundary, close to the wells, was established as a no-flow boundary according to the resistivity measurements. The highly resistive formations can act as no-flow boundaries. The geological mapping and resistivity measurements showed the reservoir to be anisotropic. The model's anisotropy is determined by the anisotropy angle and by the ratio between transmissivity in x (T_{xx}) and y (T_{yy}) directions. Due to the strike of the faults and dykes, the anisotropy angle was assumed 80° and anisotropy ratio $T_{yy}/T_{xx} = 10$. According to well tests from February and July 1982, the initial values for transmissivity were assumed to be in the range of 10^{-3} - 10^{-4} m^2/s. The transmissivity values in the shut-in tests were 3.1×10^{-4} and 2.2×10^{-4} m^2/s (Flóvenz et al., 1984).

The calibration started with the value of the storage coefficient in the range of 10^{-2} - 10^{-4}. The long term effect of the exploitation was analyzed, so the elastic storage coefficient and the delayed yield effect were taken into account. It was assumed that porosity of the reservoir is in the range of 0.01 to 0.1 and the time constant 10 - 100 days (Equation 4). The leakage coefficient was taken to be in the range of 10^{-10} - 10^{-12} s^{-1} because almost no influence on temperature from the cold water recharge from above was observed.

3.3 Results from the calibration of the reservoir parameters

The transmissivity, storage coefficient, porosity, time constant and leakage coefficient were determined by matching measured and calculated pressure values. The anisotropy angle and anisotropy ratio for transmissivity were taken as given above.

The transmissivity varies from 3.5×10^{-5} to 1.4×10^{-3} m^2/s within the area of the model. The areal distribution of the transmissivity seems to be in agreement with the resistivity map (Figures 3 and 5). The other parameters are taken as constants within the total area of the model. They are as follows:

anisotropy angle	*- 80°*
anisotropy ratio T_{yy}/T_{xx}	*- 10*
storage coefficient S	*-* 1.0×10^{-4}
effective porosity φ	*- 0.012*
time constant κ	*- 20 days*
leakage coefficient k/m	*-* 3.0×10^{-11} s^{-1}

A quite good fit between measured and calculated drawdown values was obtained with the model. The best results were obtained for production well Gy-7 (Figure 6) and a little worse in well Gy-5 (Figure 7). In well Gy-8 there were no continuous measurements of the drawdown. The first part of the exploitation period showed that the response in well Gy-8 was different from the responses in Gy-7 and Gy-5 but the model seems to fit fairly well according to Figure 8. Figure 9 shows the areal distribution of drawdown after 10 years of production. The significant changes in the water level are found at a distance less than 4 km from the production well to the north and to the south and less than 2 km to the east. The cross-section (Figure 10) also shows the rapid drawdown in the close vicinity of the wells. The arrows on the map in Figure 9 show intensity of flow and its direction.The log-log graph describes intensity of flow (Darcy velocity multiplied by the aquifer thickness) on the y-axis as a function of arrow length on the x-axis.

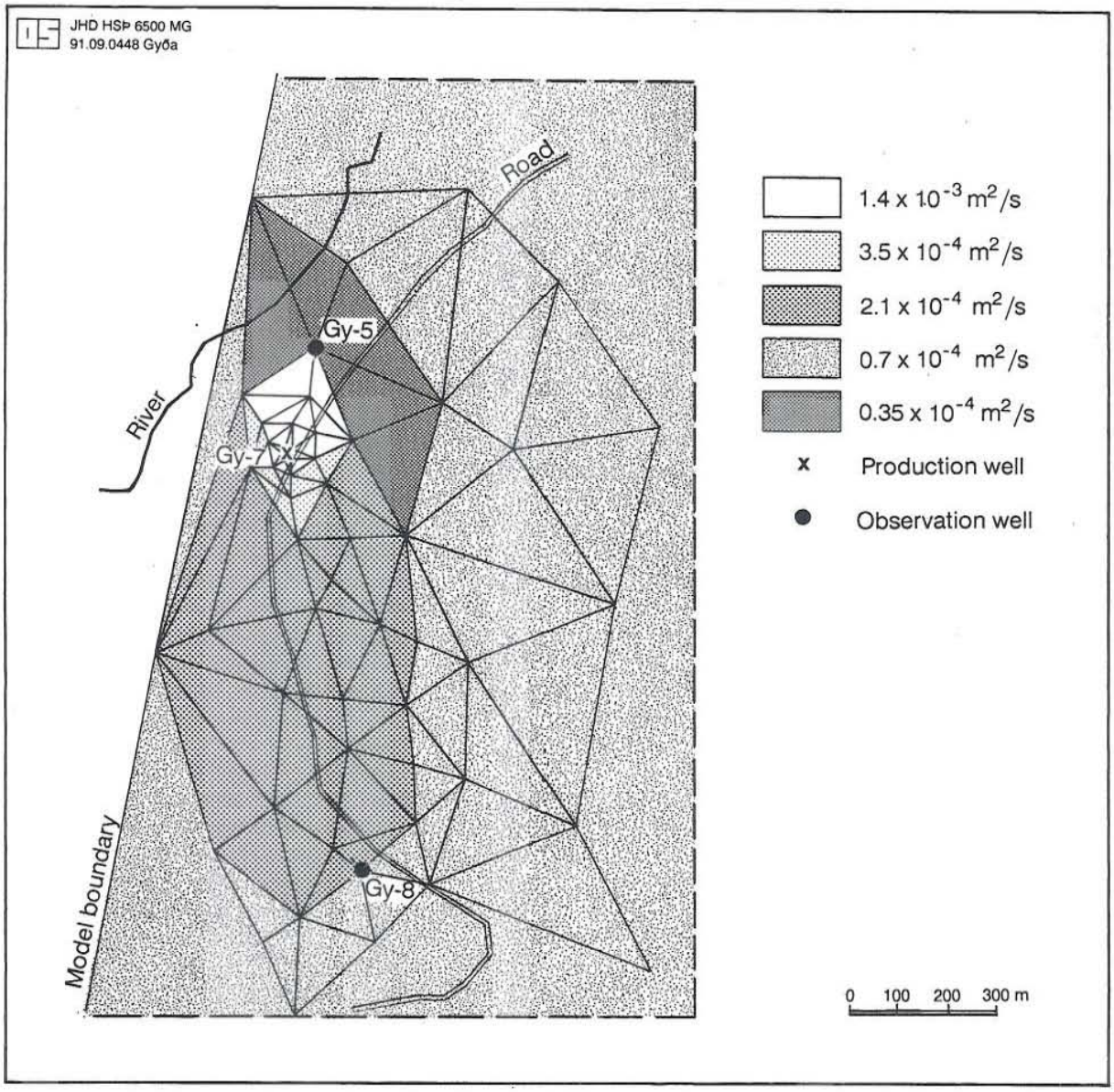

FIGURE 5: Map of transmissivity in the vicinity of wells

Several measurements of silica concentration exist from well Gy-7. The silica content decreased due to the production and the induced leakage from above. The concentration calculated with the model shows the same decreasing trend (Figure 11). As was mentioned previously, the temperature of the geothermal water is 60-61°C. Assuming the initial temperature of the water to be 60°C and the temperature of the vertical inflow to be 20°C, no cooling was observed in the model. The decline of temperature is about 0.1°C after 10 years of production.

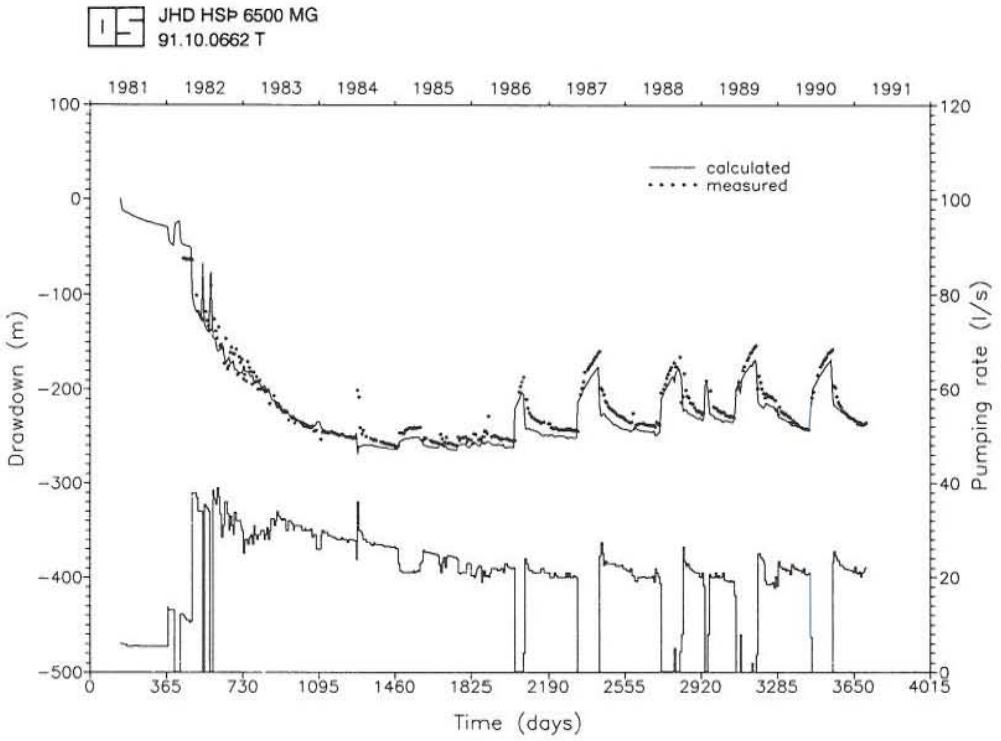

FIGURE 6: Measured and calculated drawdown, well Gy-7

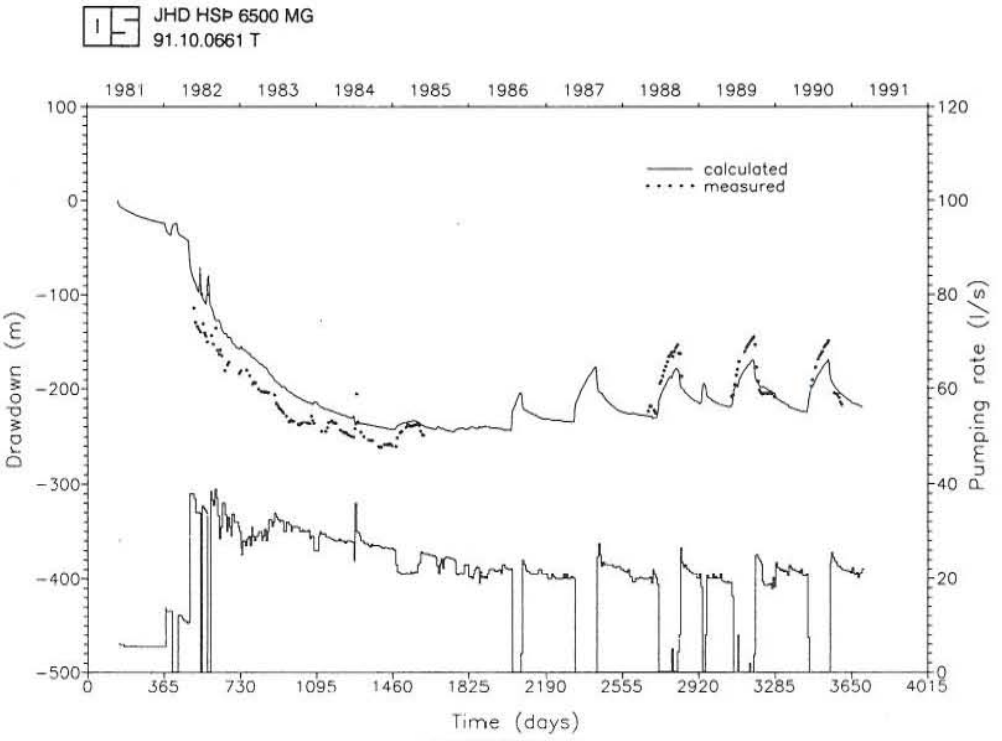

FIGURE 7: Measured and calculated drawdown, well Gy-5

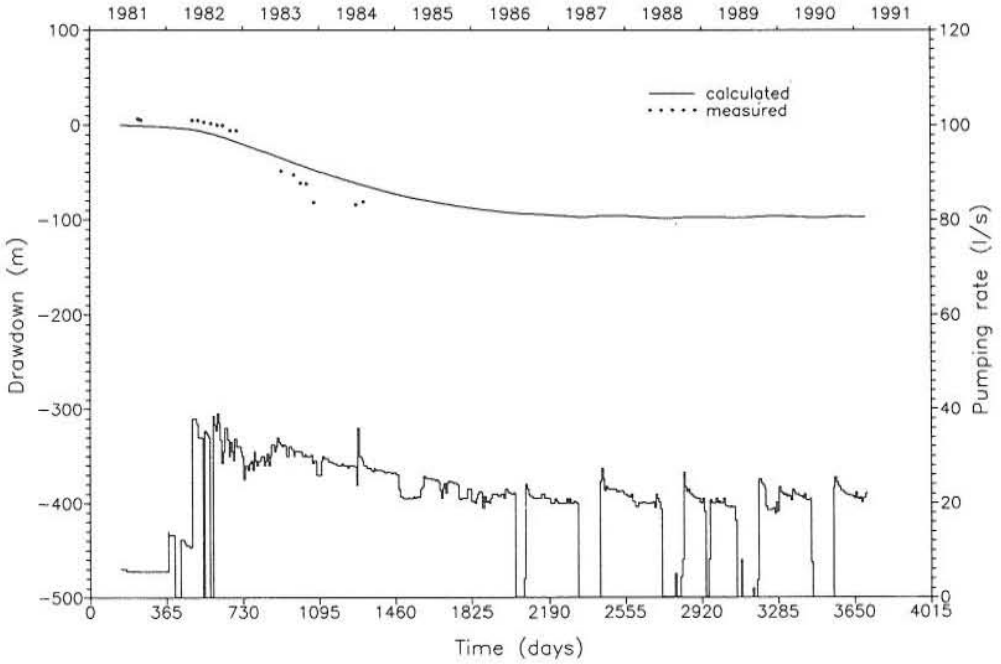

FIGURE 8: Measured and calculated drawdown, well Gy-8

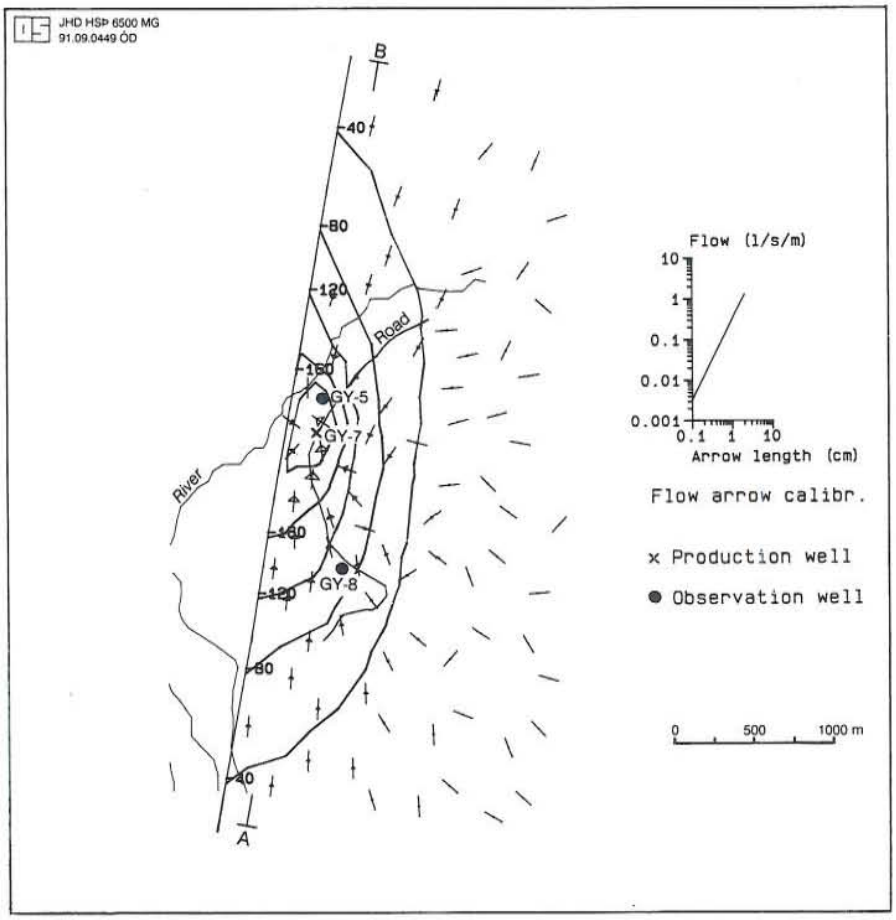

FIGURE 9: Drawdown and flow field in the vicinity of the wells

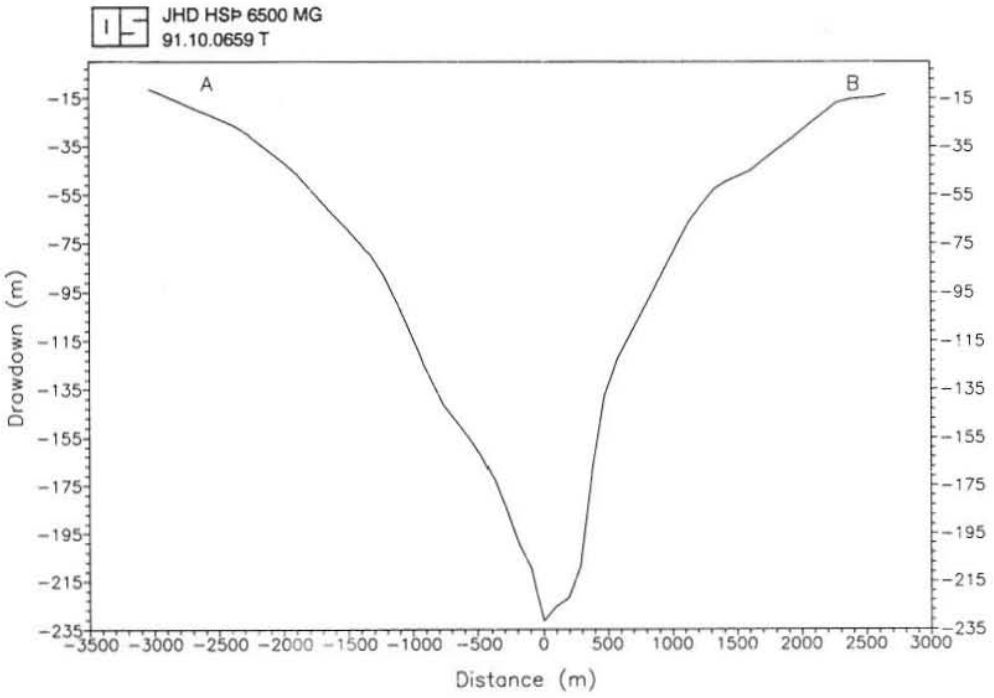

FIGURE 10: Cross-section of the drawdown

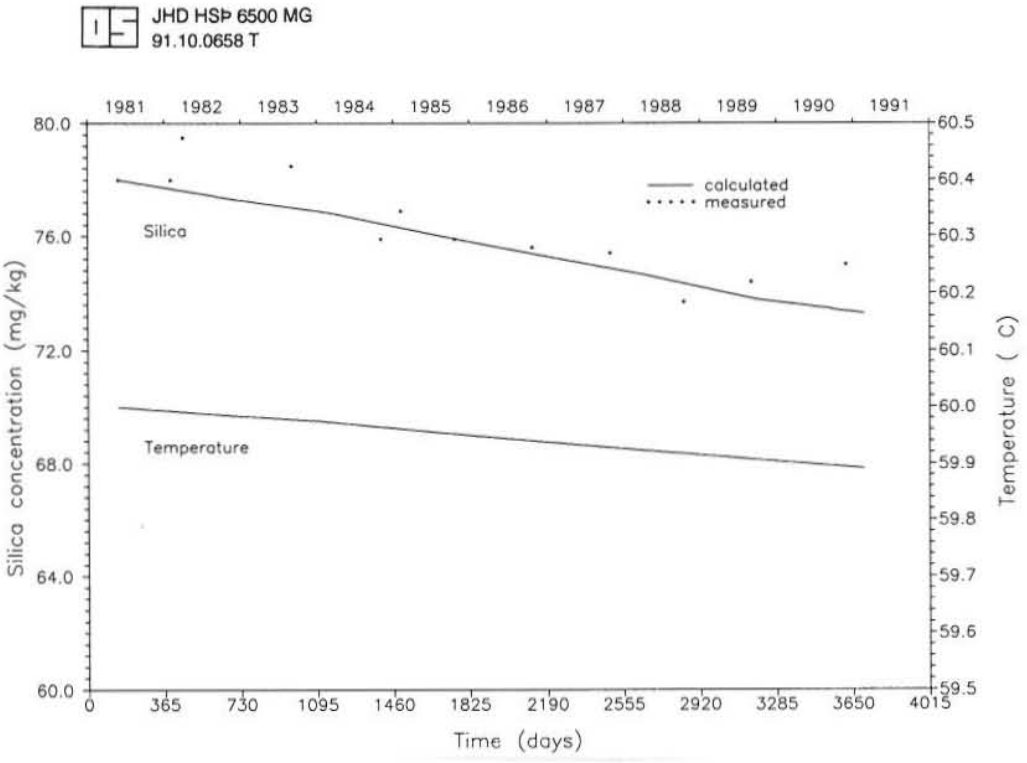

FIGURE 11: Silica concentration and temperature decline in well Gy-7

3.4 Future prediction of the reservoir response

After calibration the model was used for calculations of the drawdown until the end of year 2005. The calculations were made for different constant production rates. The results are shown in Figures 12, 13 and 14 for wells Gy-7, Gy-5 and Gy-8, respectively. The present trend of the stabilized drawdown can be kept only for a production rate not larger than 15 l/s. For the other rates, 20, 25, 30 l/s, the drawdown shows a decreasing trend. The prediction results obtained with a lumped parameter model are similar to those above (Axelsson et al., 1988 and 1989).

Future prediction for silica concentration shows the same decreasing trend as during the production period (Figure 15). The temperature prediction is very promising. It seems that there is enough heat flow in the reservoir to maintain the temperature of the water close to the initial value. The temperature decline for the highest production rate, 30 l/s, is only 0.4°C (Figure 16).

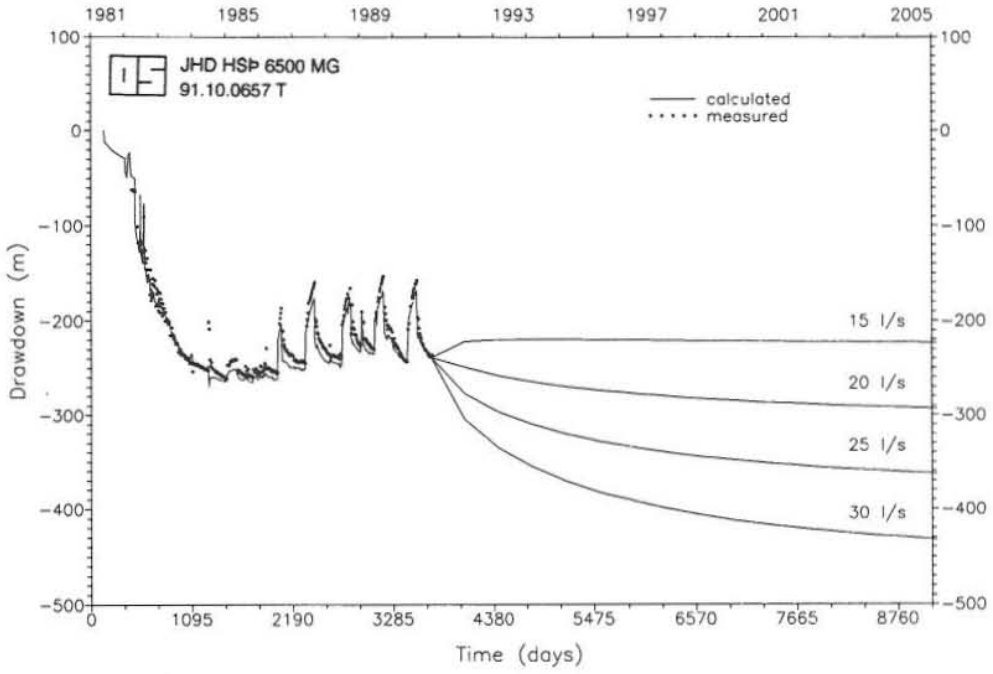

FIGURE 12: Future prediction of the drawdown, well Gy-7

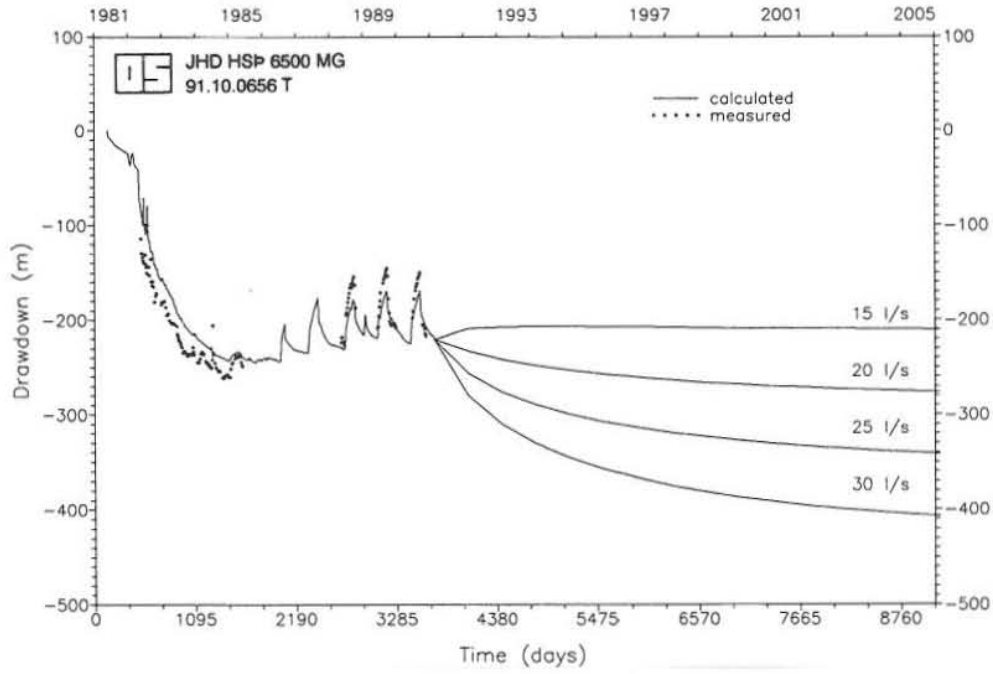

FIGURE 13: Future prediction of the drawdown, well Gy-5

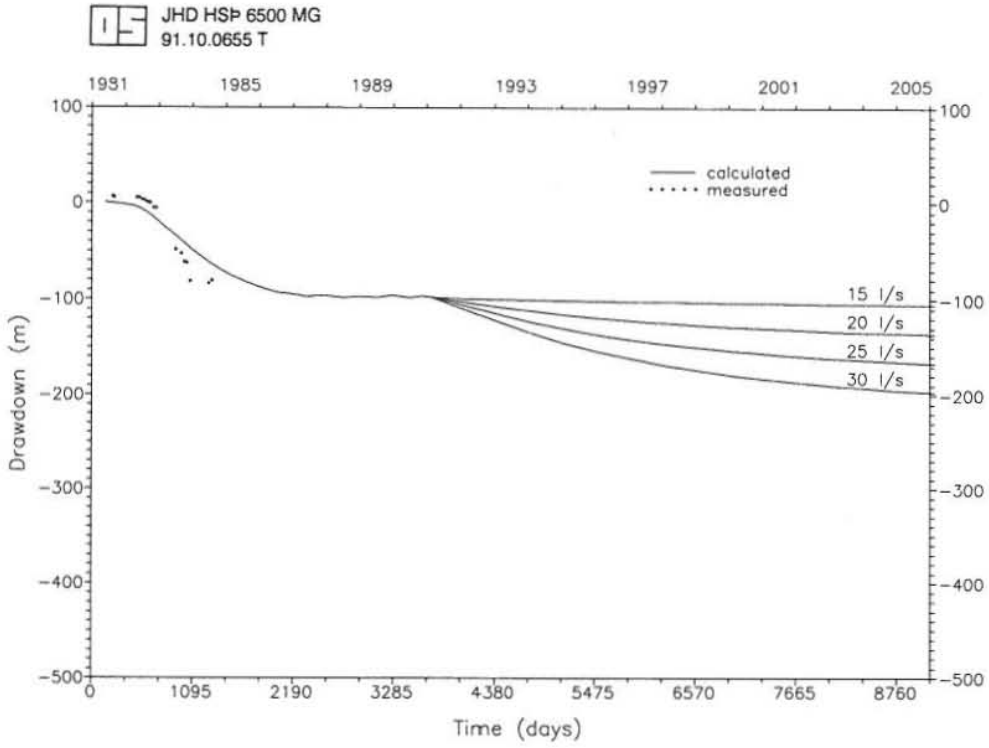

FIGURE 14: Future prediction of the drawdown, well Gy-8

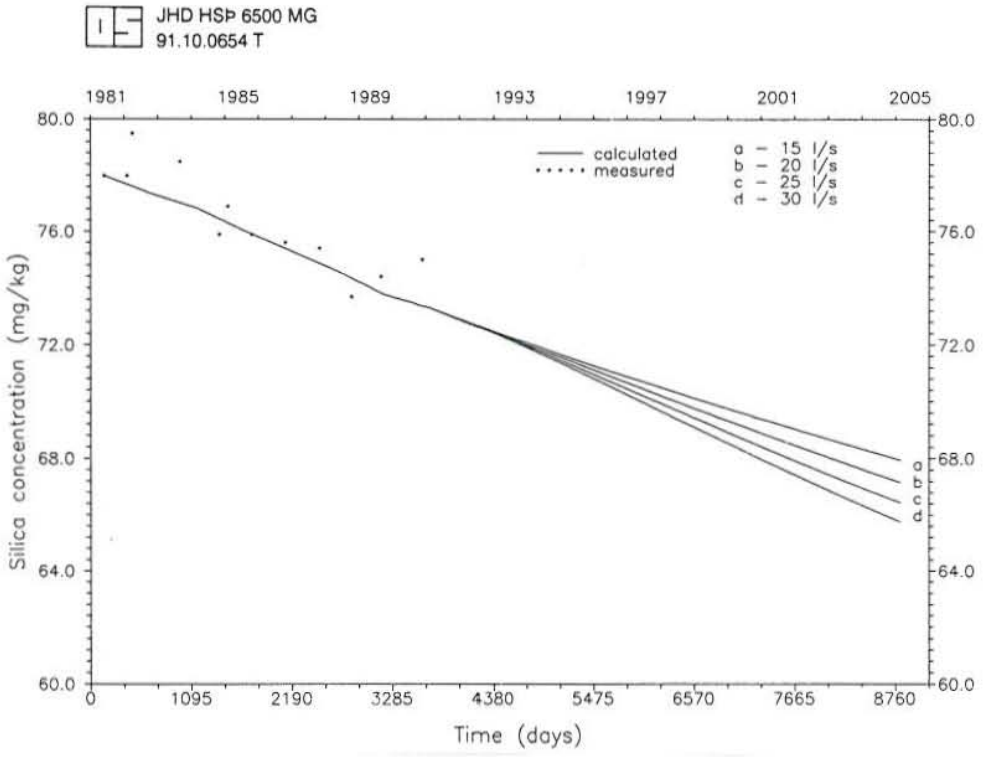

FIGURE 15: Future prediction of the silica concentration, well Gy-7

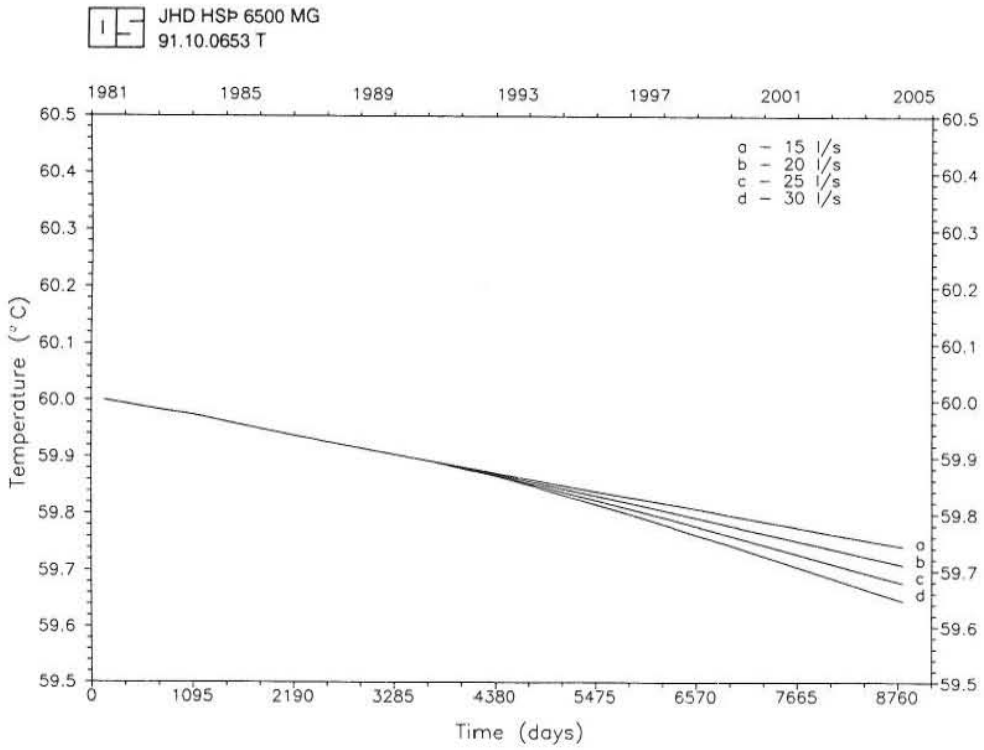

FIGURE 16: Future prediction of the temperature, well Gy-7

3.5 Conclusions and recommendations

During the last years of the production period, the reservoir has reached relatively steady-state conditions for an average annual pumping rate of between 13.5 and 15.9 l/s. Assuming future production does not exceed the present levels, the drawdown in the reservoir will not increase.

Reinjection might be another alternative for maintaining reservoir pressure, but because of the low reservoir temperature it would probably not be the best solution.

The good fit with the model for drawdown, using the equation for delayed yield, shows that the reservoir is controlled by two different storage mechanisms. At the start of production, storage is controlled by liquid/formation compressibility and in later production periods, it is controlled by the mobility of the free surface.

The modelling was based on observations close to the production well and the results show that the radius of influence is about 4 km. Continuous measurements of the water level farther away from the production zone might be used to check the model results.

4. THE PODHALE GEOTHERMAL FIELD

4.1 Main features of the Podhale geothermal field

4.1.1 Locality

The Podhale geothermal field is located in the southern part of Poland, north of the Tatra mountains. This field is a part of the Carpathians. The total area of the geological unit is about 1000 km^2, but only the central part, some 475 km^2, belongs to Poland. This region is very important for tourism and recreation (Figure 17).

FIGURE 17: General location of the Podhale geothermal field

4.1.2 Geology

The Podhale subbasin is a part of the Inner Carpathian Basin, the geological unit of the alpine orogene. It is built mainly of Mesozoic carbonates and clastic sediments covered discordantly with Paleogene carbonate and flysch formations. The basin is an asymmetric unit. It is closed tight towards the north by the Pieniny Klippen Belt and open southwards. Thus, the water loss from the reservoir may be made up with recharge from the surface (Figure 18). The aquifer has been located in the Middle Eocene nummulitic limestones and Mesozoic deposits. Due to the structure of the basin, the outflow of water is controlled by artesian pressure.

4.1.3 Exploration and development history

The first manifestation of geothermal activity in the Tatra and Podhale region was recognized in the 19th century, when a natural spring with a constant temperature of 20°C was found. In 1963 the first deep exploration well was drilled. An artesian outflow of water with a temperature of 35°C was obtained. At present, this well supplies about 14 l/s of water to the bathing pools. During the 1970's, several shallow wells were drilled in the southern part of the basin.

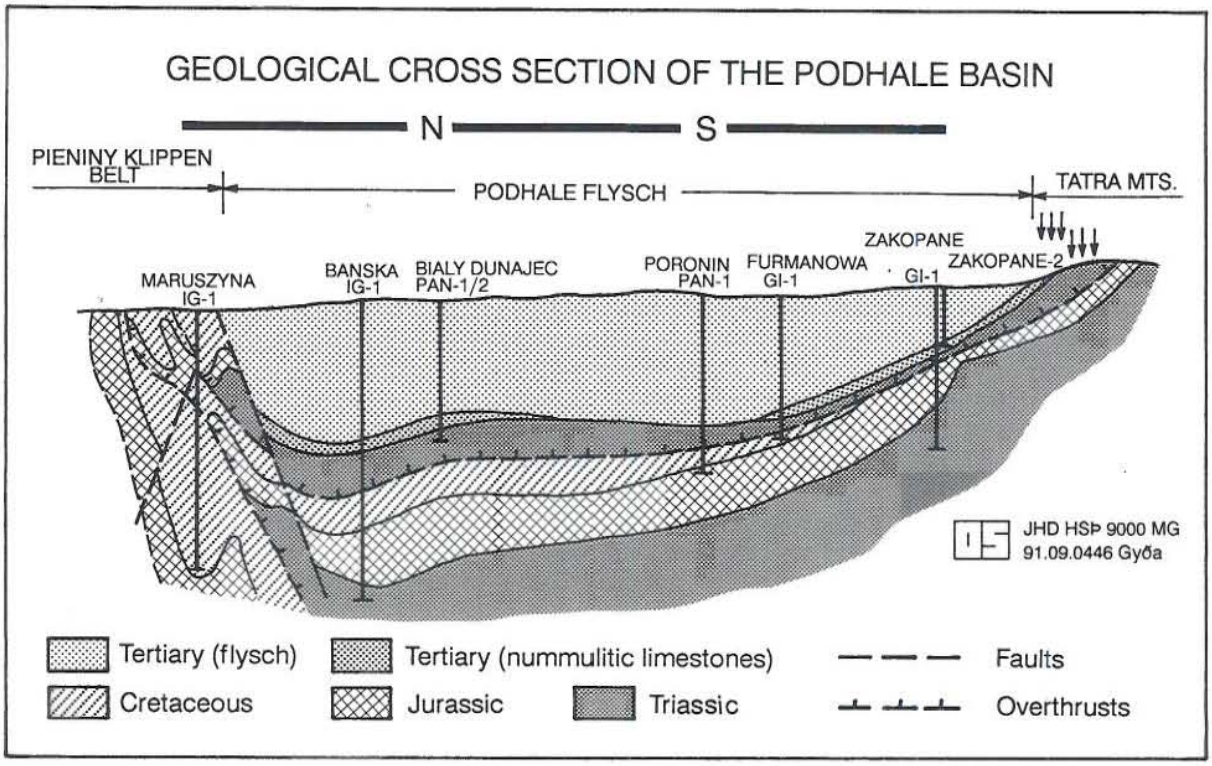

FIGURE 18: A simplified geological cross-section of the Podhale basin (based on Sokolowski, 1989)

The greatest step in geothermal development was taken when the Banska IG-1 well was completed in 1981. In this well, the artesian aquifer was recognized at a depth of 2560-2683 in the Middle Eocene limestones. Because of further drilling to a total depth of 5261 m, this horizon was cemented. In 1982, production started with 17 l/s of water with a temperature of 72°C and a wellhead pressure of 19 bars. The mineralization of the water is very low, 3021.9 mg/l (Sokolowski, 1988).

During the following 10 years, five exploration wells were drilled within the geothermal field. The temperature of the water reached 86-89°C at the wellhead.

Actually two wells, Banska-IG 1 and Bialy Dunajec PAN-1, are connected by a temporary pipeline and they are operated as the experimental geothermal doublet. The pipeline consists of three uninsulated pipes of diameter 2 7/8" each and are 1200 m long. The well Banska IG-1 produces 20 l/s of 86°C water with artesian pressure. After cooling in the pipeline on the surface, the water flows by itself down into the Bialy Dunajec PAN-1 well, which serves as the injection well.

4.2 Basic assumptions of the Podhale model parameters

On the basis of the geological structure, several doublets are planned in the area. So far there is little information on the reservoir properties because only short term well tests have been performed. The rapid build-up of the pressure in drillstem tests did not give any estimates of the reservoir parameters. On the other hand, the reservoir model can be very helpful in planning future tests.

In this report, parameters are believed to be chosen close to probable real values. Figure 19 shows the distribution of the transmissivity within the total area of the basin. Anisotropy of the reservoir is chosen in accordance with geological data. As the recharge area is to the south and the basin is closed to the north, a constant pressure boundary is chosen at the southern boundary and no-flow boundaries elsewhere. The reservoir formations are covered by thick impermeable layers so no leakage to the reservoir from above is possible.

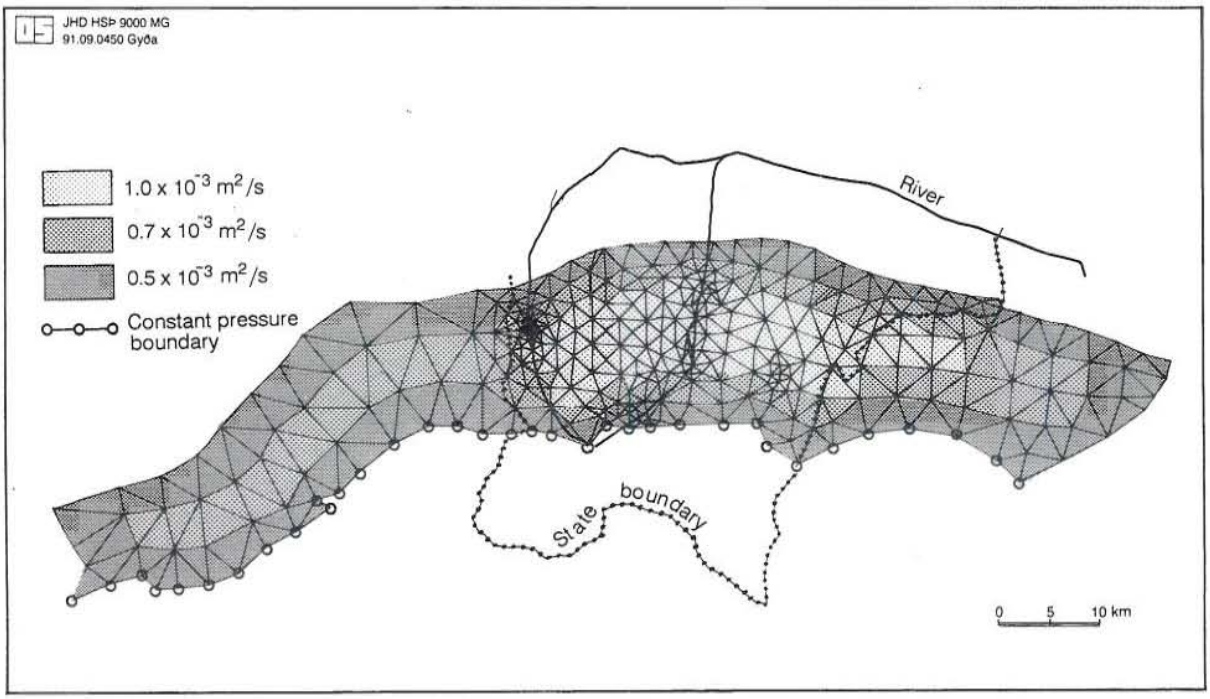

FIGURE 19: Map of transmissivity for distributed parameter model, Podhale

A stationary flow problem was solved for various constant production rates as well as the transient heat transport problem in order to determine the breakthrough time for the cold front. Because the total area is large and the wells are concentrated in the central part of the basin, a submesh was created around the examined wells for more accurate calculations. The problem was solved for two cases: a) One doublet production/injection in operation; b) Five doublets in operation (Figures 20, 21 and 25).

The assumed values of the parameters are as follows:

transmissivity T:	*0.5×10^{-3}, 0.7×10^{-3}, 1.0×10^{-3} m^2/s*
anisotropy ratio T_{yy}/T_{xx}:	*10*
anisotropy angle:	*90°*
longitudinal dispersivity a_L:	*100 m*
anisotropy ratio a_T/a_L:	*10*
porosity:	*0.05*
aquifer thickness:	*400 m*

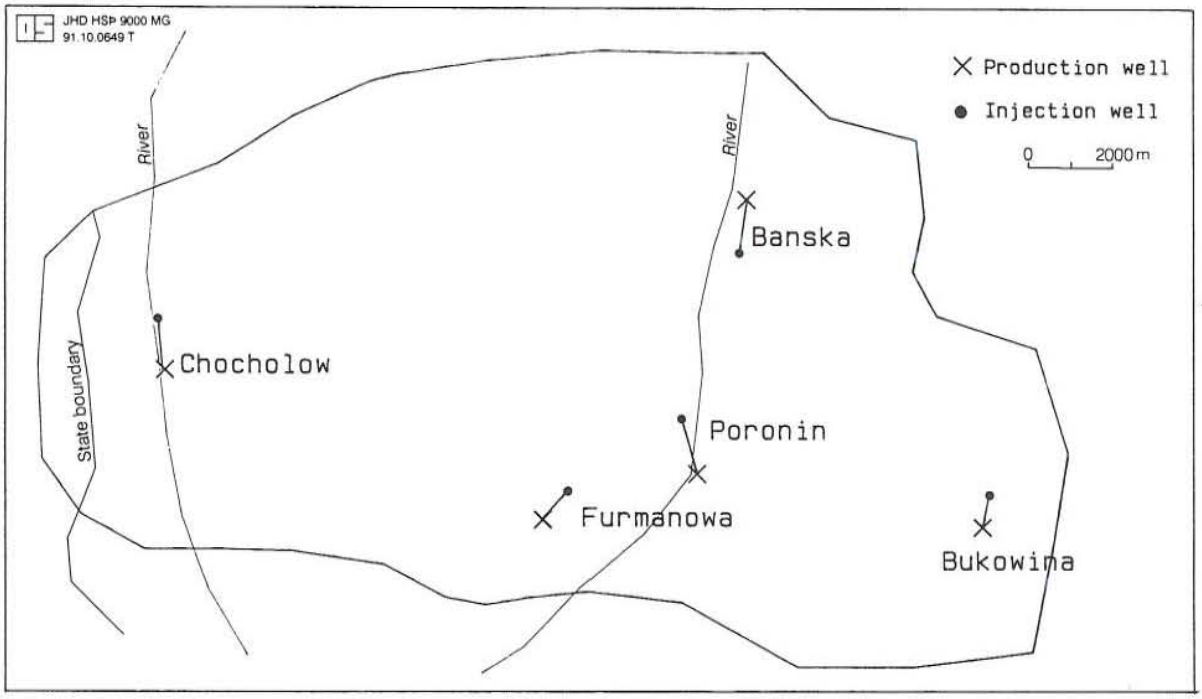

FIGURE 20: Location of wells in the Podhale model

4.3 Results from the flow model

4.3.1 The one doublet case

The doublet is located in the western part of the area; the submesh is shown in Figure 21. The distance between wells is 1250 m. The response of the reservoir was calculated for three different pumping rates:

a) 20 l/s (close to obtained artesian outflow)
b) 50 l/s
c) 100 l/s

The results from the calculations are as follows:

a) water level changes from -21.57 m in the production well to 37.03 m in the injection well, flow from 0.189×10^{-6} to 0.654×10^{-1} l/s/m.
b) water level changes from -53.93 m to 92.57 m, flow from 0.472×10^{-6} to 0.1636 l/s/m.
c) water level changes from -107.8 m to 185.14 m, flow from 0.9438×10^{-6} to 0.327 l/s/m.

Figures 22, 23 and 24 show the areal distribution of those parameters. Flow intensity and direction are shown by the arrows.

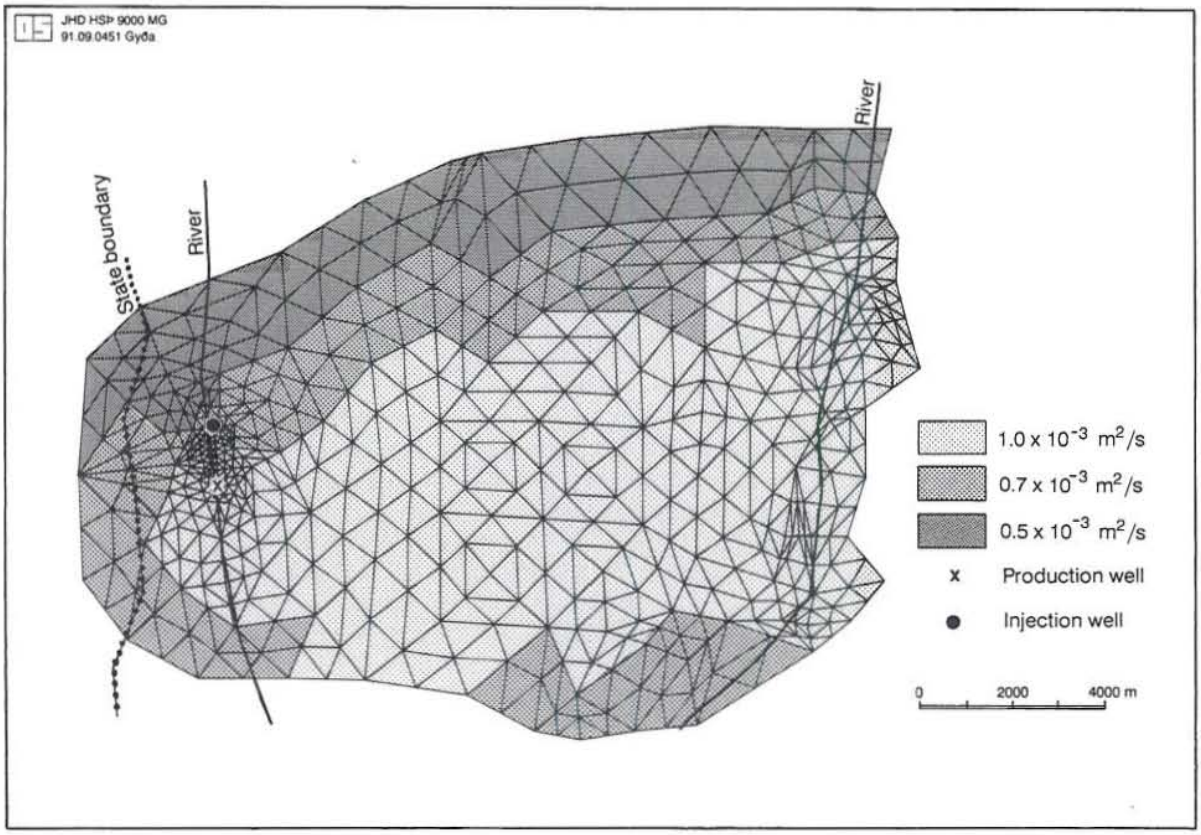

FIGURE 21: Map of transmissivity in the vicinity of the wells, case 1

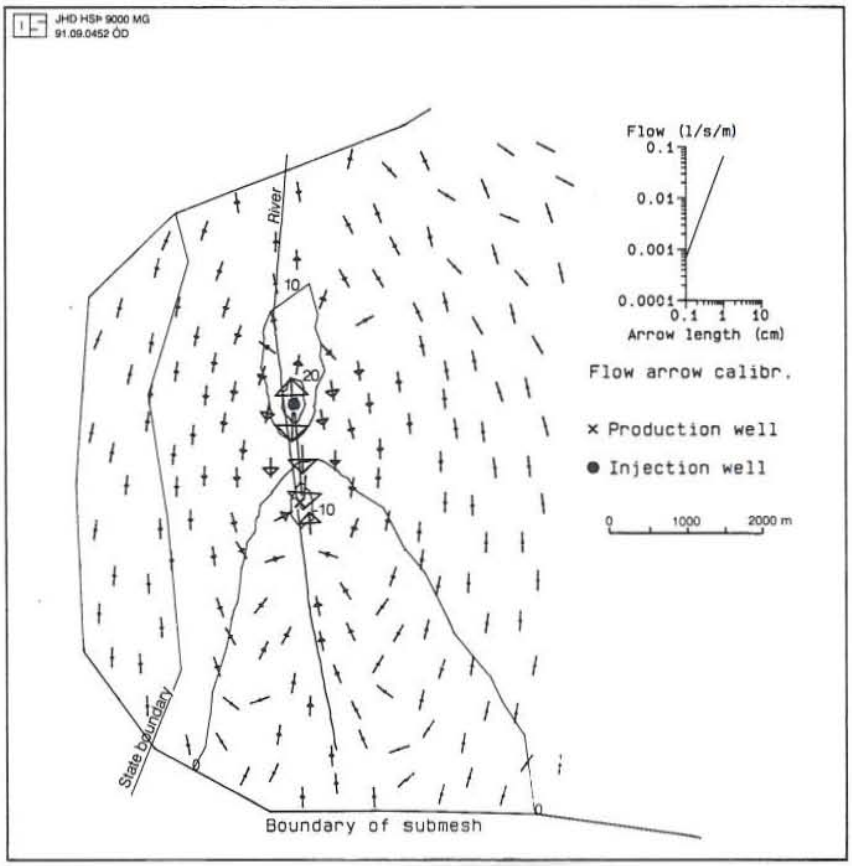

FIGURE 22: Drawdown and flow field, case 1 a

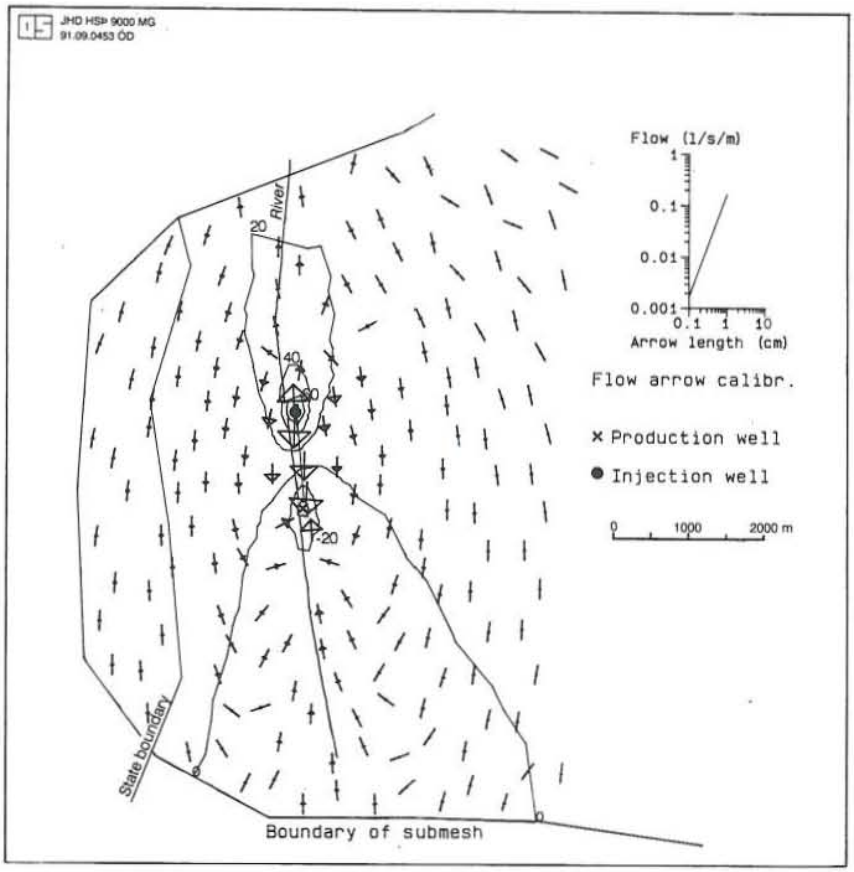

FIGURE 23: Drawdown and flow field, case 1 b

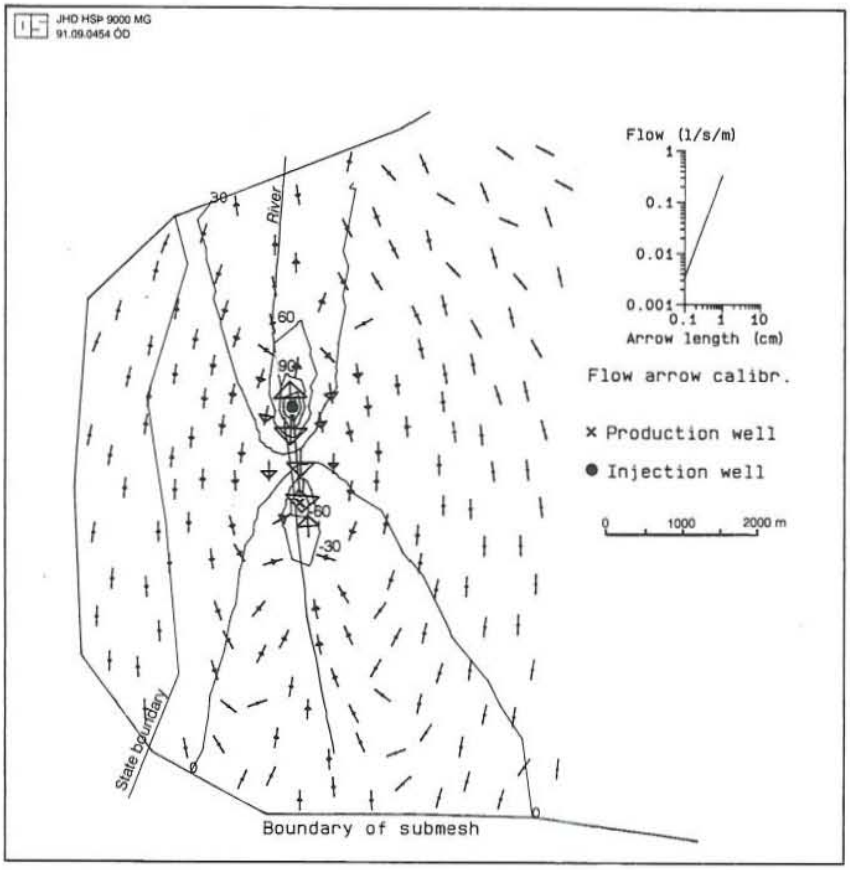

FIGURE 24: Drawdown and flow field, case 1 c

4.3.2 The five doublet case

To design future steps of utilization of the geothermal water, it is necessary to check how many production/injection doublets can be operated in the area. In this report, five doublets were considered. A new submesh was created for the calculations (Figure 25). The reservoir response was tested for two different pumping rates. The obtained results are as follows:

a) for Q = 20 l/s water level changes vary from -26.9 to 36.06 m,
flow from 0.372 x 10^{-5} to 0.08093 l/s/m.
b) for Q = 100 l/s water level changes vary from -134.5 to 180.32 m,
flow from 0.186 x 10^{-4} to 0.04046 l/s/m.

Figures 26 and 27 show the areal distribution of these parameters. The extreme values of drawdown are almost in the same range as for the one doublet case. The largest drawdown is observed in the Furmanowa production well and the largest overpressure in the Chocholow injection well.

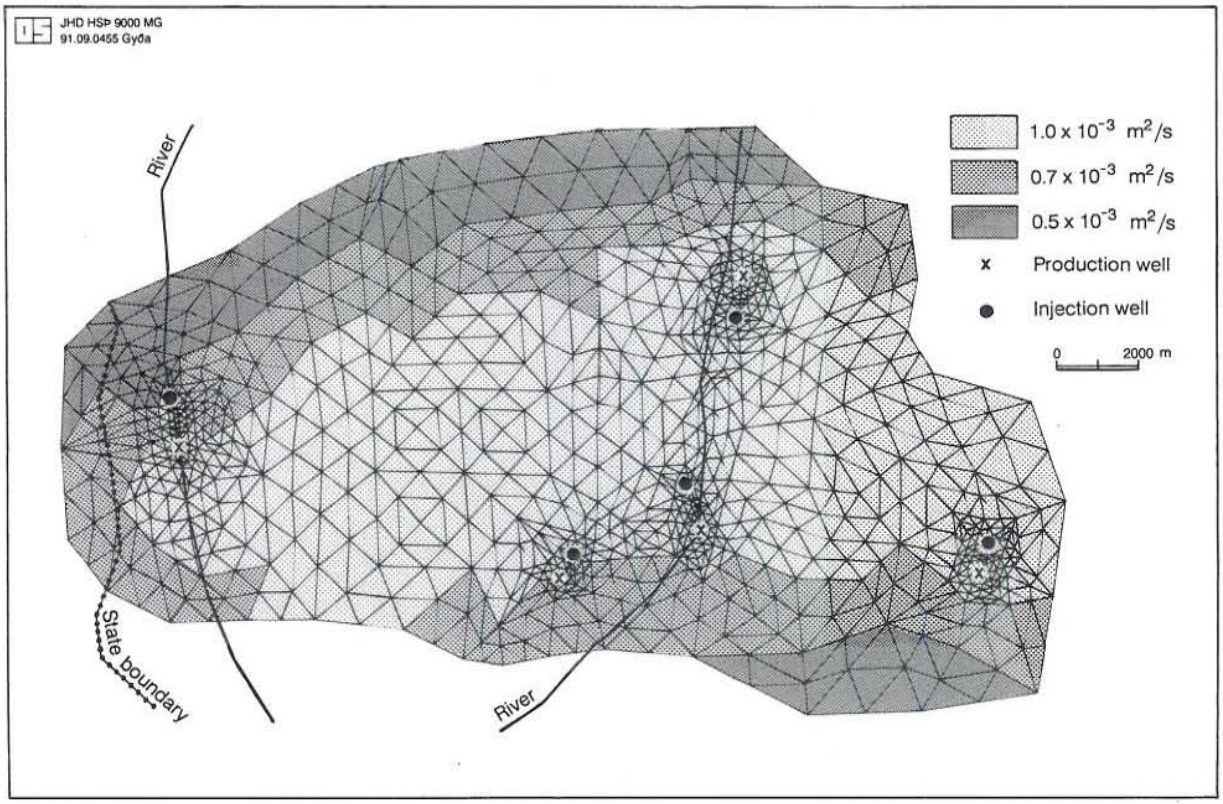

FIGURE 25: Map of transmissivity in the vicinity of the wells, case 2

4.4 Results from the heat transport model

Reinjection of geothermal waste water is a preferred way of waste disposal. Advantages of this solution consist of maintaining the reservoir pressure and protection of the environment. The danger in applying reinjection is the possibility that the cold water will break through from the injection well into the production zone. So in this model, the temperature decline was checked for both cases.

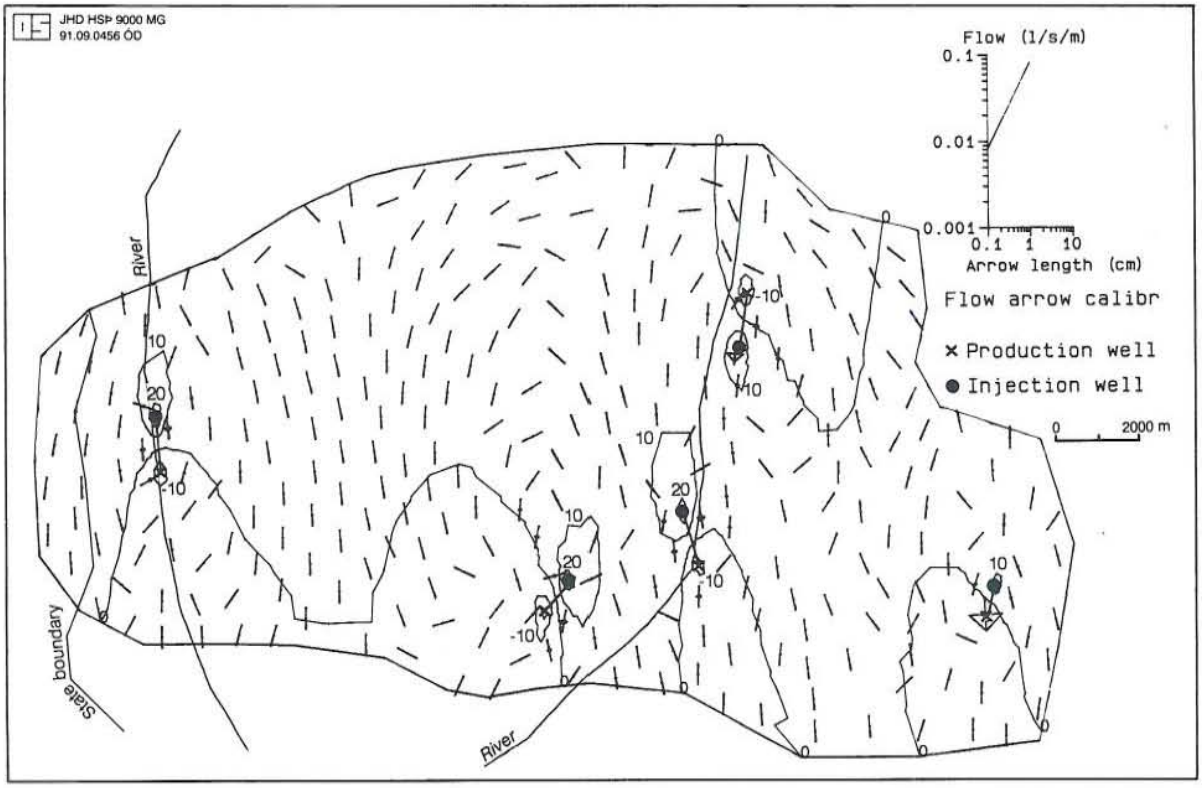

FIGURE 26: Drawdown and flow field, case 2 a

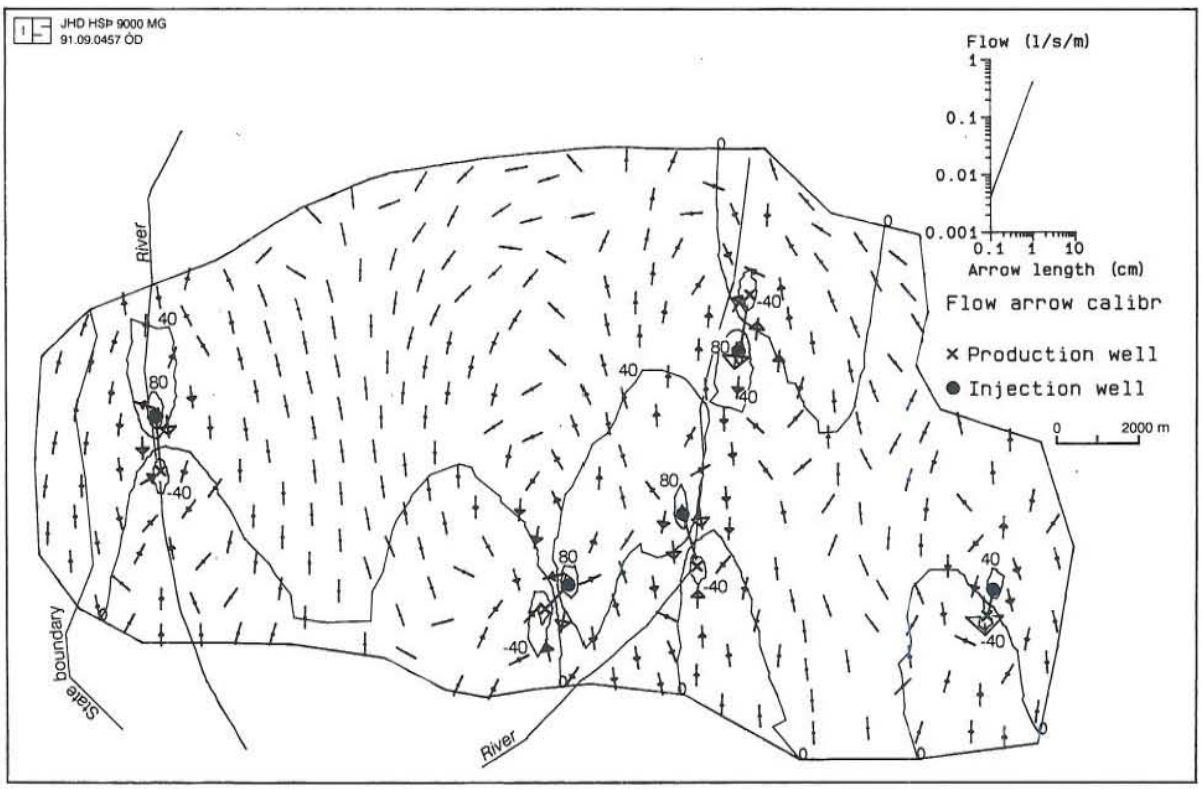

FIGURE 27: Drawdown and flow field, case 2 b

The following assumptions for the heat transport were made:

Initial temperature of geothermal water	*86°C*
Temperature of the injected water	*30°C*
Longitudinal dispersivity a_L	*100 m*
Anisotropy ratio for dispersivity a_T/a_L	*10*
Retardation constant	*0.226*
Porosity	*0.05*
Aquifer thickness	*400 m*

In case 1, one doublet in operation (Chocholow), the temperature declines for the distance between wells of 1250 m are as in Table 2.

TABLE 2: Temperature decline in production well, case 1

Injection rate (l/s)	Temperature decline after 50 years (°C)	Temperature decline after 100 years (°C)
20	0.2	1.0
50	2.0	8.0
100	8.0	20.0

High dispersivity makes the temperature decline curve very flat, especially for the smallest pumping/injection rates (Figure 28). The breakthrough time can be taken to be the time when the temperature of the pumped water reaches the average temperature of the injected water and the initial reservoir temperature. According to the assumed values, this average temperature is 58°C.

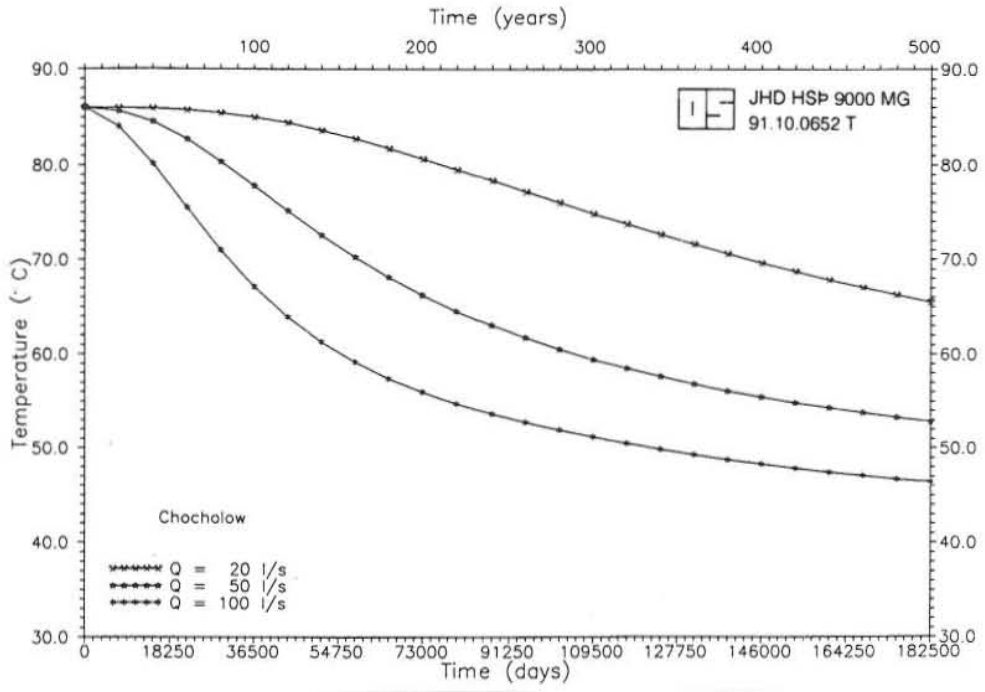

FIGURE 28: Temperature decline in production well, case 1

The time when the cold front reaches the production may be estimated by the theoretical equation for a sharp front:

$$t_{bth} = \frac{4\pi\kappa\varphi x_o^2}{3Q} \tag{17}$$

$$\kappa = 1 + \frac{(1-\varphi)\rho_s C_s}{\varphi \rho_l C_l} \tag{18}$$

where

b - *aquifer thickness (m)*
φ - *porosity*
x_o - *1/2 distance between wells (m)*
Q - *injecting rate (m^3/s)*
ρ_s - *density of porous medium (kg/m_3)*
ρ_l - *density of liquid (kg/m_3)*
C_s - *specific heat capacity of the porous medium (J/kg °C)*
C_l - *specific heat capacity of liquid (J/kg °C)*

The results of the breakthrough time calculations are shown in Table 3.

TABLE 3: Breakthrough time, case 1

Injection rate (l/s)	Time - Equation 17 (years)	Time - AQUA (years)
20	638	900
50	255	320
100	127	157

In case 2 - five doublets in operation - there are different distances between wells. They are

Banska	-1260 m
Chocholow	-1250 m
Poronin	-1256 m
Furmanowa	-900 m
Bukowina	-710 m

The temperature decline was checked for two different pumping/injection rates: 20 and 100 l/s. The results are shown in Figure 29. For a pumping/injection rate of 20 l/s, there is almost no difference between the four doublets. Only the Bukowina doublet differs from the others. For the larger rate, 100 l/s, the difference between wells is considerable. The values of the temperature decline are shown in Table 4.

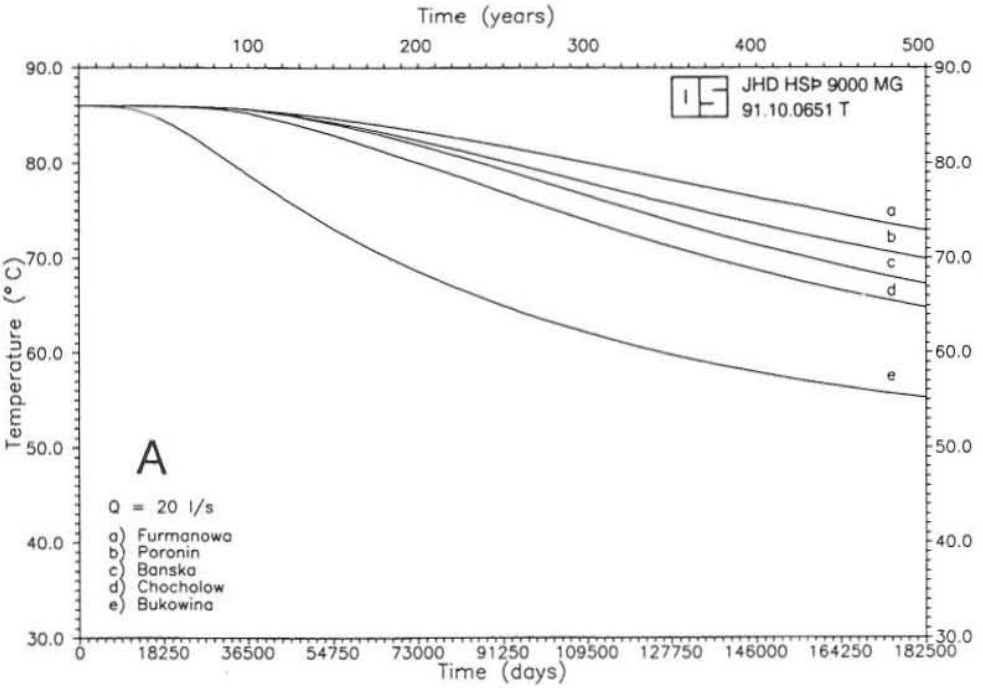

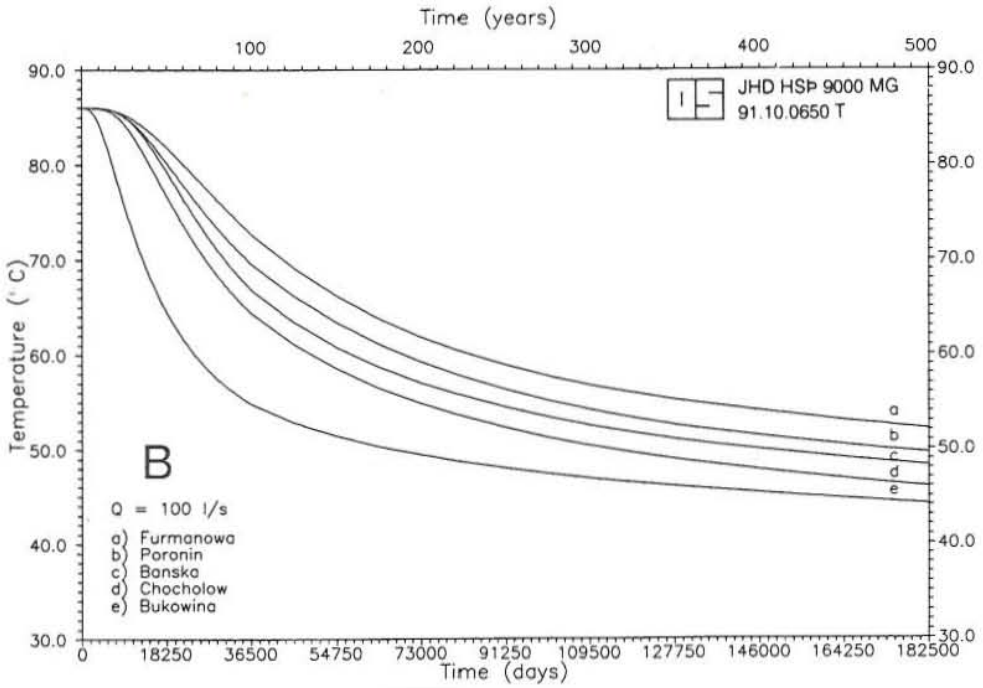

FIGURE 29: Temperature decline in production wells, case 2

TABLE 4: Temperature decline in the production wells, case 2

	Q = 20 l/s		Q = 100 l/s	
	50 years	100 years	50 years	100 years
Banska	0.02 °C	0.33 °C	6.7°C	19 °C
Bukowina	1.5 °C	7.2 °C	21.5 °C	31 °C
Poronin	0.02 °C	0.34 °C	5.8 °C	16.4 °C
Furmanowa	0.02 °C	0.32 °C	4.2 °C	13.2 °C
Chocholow	0.03 °C	0.71 °C	9.2 °C	21.6 °C

Calculations with Equation 17 and the AQUA programme give the breakthrough time due to the pumping/injection rates as shown in Table 5.

TABLE 5: Breakthrough time, case 2

	Time - Equation 17 (years)		Time - AQUA (years)	
	20 l/s	100 l/s	20 l/s	100 l/s
Banska	648	129	900	180
Chocholow	638	127	760	150
Poronin	644	129	1000	225
Furmanowa	331	66	>1000	275
Bukowina	206	41	400	77

The largest decline is observed in the doublets operating separately from others (Bukowina and Chocholow). Location of the doublets along the favourable direction of flow (transmissivity in the S-N direction is higher than in the E-W direction) is an additional reason for a higher decline in doublets (compare Banska and Furmanowa). Figure 30 shows areal distribution of temperature after 50 years for a pumping rate of 100 l/s.

4.5 Conclusions and recommendations

The theoretical reservoir model must be checked against real measurements. It is necessary to perform long term well tests. The most important parameter is the value of transmissivity.
The model shows that there is almost no difference in the drawdown depending on how many pairs of wells are in operation simultaneously. Also, if the doublets are far away from each other the decline of temperature is independent of the number of doublets. In the Chocholow doublet the same temperature decline is observed in cases 1 and 2.

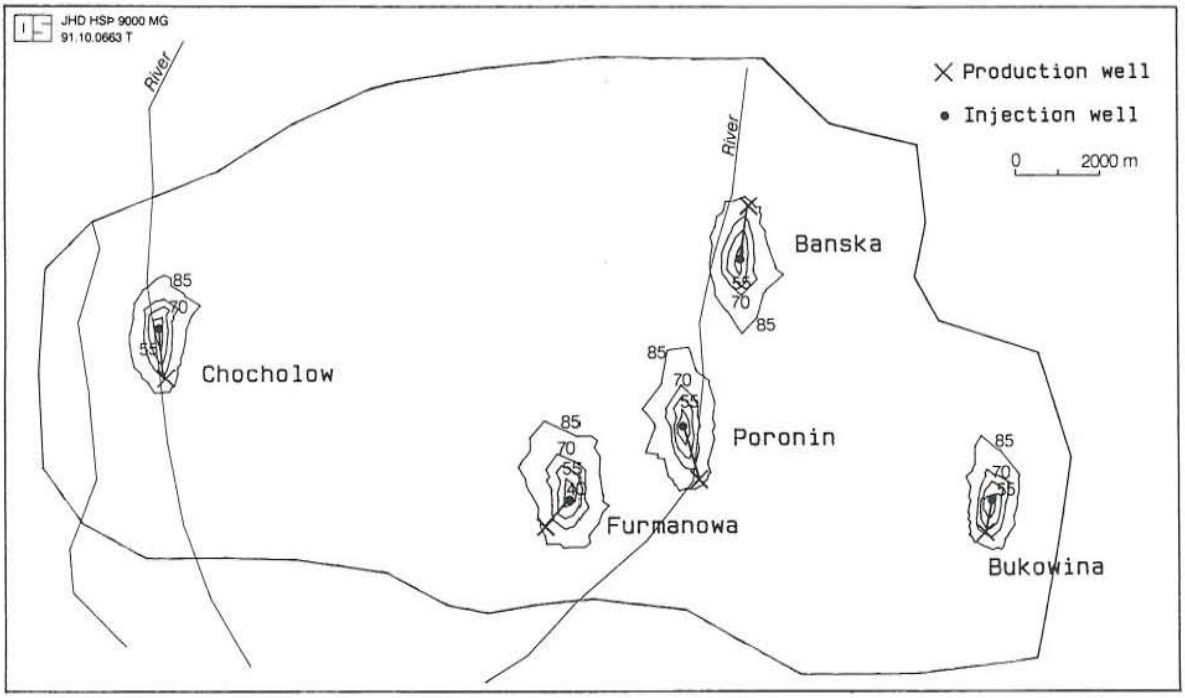

FIGURE 30: Map of temperature after 50 years of production, case 2

The proper configuration of the doublets in relation to areal transmissivity distribution and the anisotropy of the reservoir may increase the lifetime of the doublets. Therefore, before drilling new wells, it is important to test different locations of wells by way of a model.

The distance between the wells is the most important factor affecting the breakthrough time of the cold front. A distance of less than 1000 m may be insufficient to delay the cold front.

ACKNOWLEDGEMENTS

I am very appreciative to all persons who provided me with help, guidance and advice during the whole period of studying and formulating the final report. I would especially like to thank Dr. Ingvar B. Fridleifsson for giving me the chance to attend the UNU Geothermal Training Programme, Dr. Snorri Pall Kjaran, my advisor, for his assistance during the data analysis and preparation of this report and Sigurdur Larus Holm for patiently acquainting me with the AQUA programme.

Special thanks go to Dr. Einar T. Eliasson, the first Icelander I met, for recommending my application.

I also wish to extend my gratitude to the Government of Iceland and the United Nations University for the Fellowship.

I am very grateful to all lecturers for comprehensive presentations, particularly to all the staff of the Reservoir Engineering Unit for their willingness to share their knowledge and experience.

I would also like to thank Ludvik S. Georgsson for his assistance during the whole period of studies, Marcia Kjartansson for 'translating' this report into correct English, the ladies in the drawing room for completing the figures and all the staff of Orkustofnun who were kind enough to support me with technical assistance.

I would like to extend my thanks to Prof. Julian Sokolowski and Prof. Roman Ney of the Polish Academy of Sciences, who allowed me leave to attend the course.

My personal thanks go to all people who showed me the magnificent beauty of Iceland.

NOMENCLATURE

a_L - longitudinal dispersivity (m)
a_T - transversal dispersivity (m)
b - aquifer thickness (m)
c - solute concentration (kg/m^3)
c_o - solute concentration of vertical inflow (kg/m^3)
c_w - solute concentration of injected water
C_l - specific heat capacity of the liquid (kJ/kg°C)
C_s - specific heat capacity of the porous media (kJ/kg°C)
D_m - molecular diffusivity (m^2/s)
D_{xx} - dispersion coefficient in x direction
D_{yy} - dispersion coefficient in y direction
h - groundwater head (m)
h_o - head in upper aquifer (m)
k - permeability of the semipermeable layer (m/s)
K_d - distribution coefficient
m - aquitard thickness (m)
R - infiltration (mm/year)
R_d - retardation coefficient
S - storage coefficient
t - time (s)
T - temperature (°C)
T_o - temperature in vertical inflow (°C)
T_{xx} - transmissivity in x direction (m^2/s)
T_{yy} - transmissivity in y direction (m^2/s)
Q - pumping/injection rate (m^3/s)
v - velocity (m/s)
v_x - velocity vector (m/s)
v_y - velocity vector (m/s)

Greek symbols:

β_c - retardation constant (mass transport)
β_h - retardation constant (heat transport)
γ - leakage (m/s)
κ - time constant (s)
λ - decay constant (s^{-1})
ρ_l - density of the liquid (kg/m^3)
ρ_s - density of the porous media (kg/m^3)
φ - porosity

REFERENCES

Axelsson, G., 1989: Simulation of pressure response data from geothermal reservoir by lumped parameter models. Proceedings, 14th Workshop on Geothermal Reservoir Engineering, Stanford University, California, 257-263.

Axelsson, G., Tulinius, H., Flovenz, O.G., and Thorsteinsson, Th., 1988: Geothermal resources of the Akureyri District Heating System. Orkustofnun, Reykjavik, report OS-88052/JHD-10 (in Icelandic), 35 pp.

Bodvarsson, G.S., and Witherspoon, P.A., 1989: Geothermal reservoir engineering, Part I. Geothermal Science and Technology, 2-1, 1-68.

Flovenz, O.G., Axelsson, G., and Ingimarsdottir, A., 1991: Production monitoring for the Akureyri District Heating System in 1990. Orkustofnun, Reykjavik, report OS-91009/JHD-02 B (in Icelandic), 28 pp.

Flovenz, O.G., Einarsson, S., Gudmundsson, A., Thorsteinsson, Th., and Kristmansdottir, H., 1984: Geothermal exploration in Glerardalur from 1980 to 1983. Orkustofnun, Reykjavik, report OS-84075/JHD-13 (in Icelandic), 89 pp.

Sokolowski, J., 1988: Occurrences of geothermal waters in Poland and their utilization program in Podhale region, (in English). Technika Poszukiwan Geologicznych, Geosynoptyka i Geotermia, 1-2, 49-58.

Sokolowski, J., 1989: Geosynoptical cross-section along the line Nowy Targ-Zakopane, (in Polish). Report CPBR 5.2 cel 15.B, Polish Academy of Sciences - Minerals and Energy Economy Research Centre, Cracow.

Vatnaskil Consulting Engineers, 1990: AQUA, user's manual. Vatnaskil, Reykjavik.